KTH Land and Water Resources Engineering

NUMERICAL MODELING OF A SLOTTED FLIP BUCKET SPILLWAY SYSTEM - THE SHIBUYA HYDROPOWER PROJECT

Johan Axelsson & Roger Knutsson

March 2011

TRITA-LWR Degree Project
ISSN 1651-064X
LWR-EX-11-06

Degree Project for the Master's Program in Civil Engineering

Hydraulic Engineering

Department of Land and Water Resources Engineering

Royal Institute of Technology (KTH)

SE-100 44 STOCKHOLM, Sweden

Reference to this publication should be written as: Axelsson, J, Knutsson, R (2011) "Numerical modeling of a slotted flip bucket spillway system – The Shibuya Hydropower Project" TRITA LWR Degree Project 11:06

SUMMARY

Modern computational fluid dynamics, CFD, was introduced to the aircraft industry in the mid 1900's and has expanded to many other fields of engineering since then. CFD is today a useful tool in many hydraulic projects. There are, however, still uncertainties about where CFD is a fully reliable tool and scale models are still used to verify CFD results in large and complex hydraulic structures.

The aim of this degree project is to verify scale model investigations of the spillway system of the Shibuya Hydropower Project and to find some hydraulic properties, namely: which of the five spillway channels have the best discharge capacity, the pressure distribution along the spillway channels and to find the throw distance from the flip buckets.

To decide whether the spillway channels could be modeled separately or had to be modeled together and what kind of mesh density was needed, five models were investigated. It was found that individual modeling using symmetry gave the same results as when all five channels were modeled together, thus the individual symmetry model was chosen due to much denser mesh.

When geometry and mesh was chosen the settings in the CFD software, FLUENT, was evaluated. In order to validate the settings, eight modifications were tested on the same model and the results indicated that the settings used when geometry and mesh layout was chosen were good.

The numerical and scale model results gave similar results in discharge capacity when all channels were modeled together. When the channels were modeled separately no significant difference in discharge capacity could be found among the channels but it can be noted that the separately modeled spillway channels had higher discharge capacity than when all channels were modeled in the same model.

In general there was low agreement between the scale model and the numerical pressure distribution. However, in the beginning and in the end of each channel the agreement was considered acceptable. No negative relative pressures were found in the numerical results, as were present in the scale model results.

It was found that the jet flow throw distance was quite the same for Channel 2-5 and a bit shorter for Channel 1. The span is shortest for Channel 5 and the velocity of the jet at the outlet of the spillway channels was the highest in Channel 1.

The results from this degree project indicate that there still are issues concerning agreement between scale models and CFD. The importance of having qualitative verification data in the form of several hydraulic parameters and making an analysis of required discretization level cannot be stressed enough.

SUMMARY IN SWEDISH

Modern ”computational fluid dynamics” (CFD; på svenska beräkningsbar strömningsdynamik) började i mitten av 1900-talet att användas inom flygplanskonstruktion och användandet har sedan dess spridit sig till många andra områden. CFD är i dag ett användbart verktyg i många projekt där hydrauliska beräkningar ingår. Det finns dock fortfarande osäkerheter om när CFD är ett tillförlitligt verktyg och fysiska skalmodeller används fortfarande för att bekräfta CFD-resultat i stora och komplexa hydrauliska system.

Syftet med detta examensarbete är att bekräfta resultat från en skalmodell av utskoven hos vattenkraftanläggningen Shibuya Hydropower Project och att bestämma vissa hydrauliska parametrar, nämligen: vilken av de fem avbördningskanalerna som har den bästa avbördningsförmågan, den statiska tryckprofilen längs avbördningskanalernas längd och kastlängden från skidbackarna i slutet av kanalerna.

För att avgöra om avbördningskanalerna kan bli modellerade individuellt eller om de är tvungna att modelleras tillsammans och vilken celldensitet som är nödvändig, skapades fem modeller. Det visade sig att individuell modellering gav samma resultat som när alla avbördningskanaler modellerades samtidigt. Därmed valdes individuell modellering på grund av den högre celldensiteten.

När geometri och cellstruktur var vald utvärderades inställningarna i CFD-programvaran FLUENT. Åtta olika modifikationer av inställningarna kördes i samma modell och resultaten indikerade att inställningarna som användes vid bestämmande av geometri och cellstruktur var acceptabla.

Resultaten från de numeriska modellerna och skalmodellen gav liknande resultat gällande avbördningskapaciteten när alla avbördningskanaler modellerades samtidigt. När kanalerna modellerades individuellt upptäcktes ingen signifikant skillnad i avbördningskapacitet kanalerna sinsemellan men noterbart är att de individuellt modellerade kanalerna hade en högre avbördningsförmåga än när alla kanaler modellerades samtidigt.

Generellt sett var överensstämmelsen låg mellan den numeriska modellens och skalmodellens tryckfördelning. Acceptabel överensstämmelse kunde dock observeras i början och slutet av varje kanal, men inte i de mellersta delarna. Inga negativa relativa tryck påträffades i de numeriska simuleringarna, vilket var fallet i resultaten från skalmodellen.

Kastlängden från skidbackarna var i princip densamma för Kanal 2-5 men lite kortare för Kanal 1. Strålen från Kanal 5 hade minst spridning i längdriktningen och vattenhastigheten vid utloppen var högst för Kanal 1.

Resultaten från detta examensarbete indikerar att det fortfarande finns problem med överensstämmelse mellan skalmodeller och CFD. Vikten av att tillgå kvalitativ verifieringsdata i form av ett flertal hydrauliska parametrar och att analysera erforderlig diskretiseringsnivå, kan inte tillräckligt påpekas.

SUMMARY IN CHINESE

在20 世纪中期现代计算流体力学(CFD)就已应用到了航空业，随后应用扩展到许多其他工程领域。如今CFD已是许多水利工程的有用工具。但是，作为一个完全可靠的技术，CFD 还有不确定性。大型复杂的水利工程结构的CFD 结果还需要用比例模型来验证。

此篇论文的研究目的是验证水布垭水电站泄洪系统的比例物理模型的使用，同时并揭示一些水力特性，即: 五个泄洪道中哪个具有最佳的泄洪能力，沿着泄洪道的压力分布和水流从挑坎挑出的挑距。

为了确定是否泄洪道模型能各个溢洪道各自建模或所有溢洪道一起建模，及需用什么种类的计算网格密度，我们对5个模型进行了研究。结果发现：考虑溢洪道对称性而建立单一模型所取得的结果与五个溢洪道一起所建立模型所得到结果一样。因此，由于实际模拟中用到更密的网格，在论文中我们使用单一对称模型。

当选定好单元几何形状和网格时，可评估CFD软件中的各项参数设置。为了验证各参数设置的可行性，在同一个模型上我们进行了8 次修改。结果表明，在论文中当选定好几何形状和网格布置时使用的参数设置是很好的。

当把所有的泄洪道一起建模时，在泄洪能力上数值结果和由比例物理模型所获得的结果是一样的。当使用单一溢洪道建模时，发现各个泄洪通道的泄洪能力没有太大的区别。但可以看到的是，单一建模所得到的泄洪能力要比所有溢洪道一起建模的能力要大。

一般情况下，由比例物理模型所获得的溢洪道压力分布结果与数值结果吻合得不太好。然而，每个泄洪道进口和出口处的压力分布结果两者吻合较好。正如在比例物理模型中所阐述的，在大量的数值结果中，并没有负相对压力的数值。

建模结果还表明，第2–5溢洪道的射流挑距离是一样的，而第1溢洪道的挑距与其它的相比要稍短。第5溢洪道的长度最短，而在所有溢洪道中出口射流速度最高的在第1溢洪道的

本学位项目中的结果表明：比例物理模型和 CFD 所获得结果还存在一致性的问题。数个水力参数的数据定性验证和所要求离散程度的分析的重要性没有足够的强调。

ACKNOWLEDGEMENTS

The study was carried out at Tsinghua University, Beijing, China and is part of an ongoing cooperation between Tsinghua University, Elforsk AB (the R&D organization of the Swedish power companies) and the leading universities of technology in Sweden. The purpose of the project is to provide Swedish students with international experience in the hydropower field.

We would like to thank the financial sponsors of this degree project, namely: Elforsk AB and the Department of Land and Water Resources Engineering at the Royal Institute of Technology.

We also want to thank Professor Yong Liang Zhang and Associate Professor Li Ling at the Department of Hydraulic Engineering at Tsinghua University in Beijing for their help during our stay in China.

We would further like to thank Dr. James Yang at Vattenfall R&D for taking care of all arrangements concerning our stay in China and for valuable help about modeling.

We would like to thank our adviser and examinator Hans Bergh at the Department of Land and Water Resources Engineering at the Royal Institute of Technology.

At last, Johan would like to thank Stina Banck for allowing him go to China and do his degree project.

ABBREVATIONS

CFD Computational fluid dynamics.

CFRD Concrete faced rockfill dam.

DES Detached eddy simulation.

DNS Direct numerical simulation.

EXP The scale model experiment.

FVM Finite volume method.

LES Large eddy simulations.

RANS Reynolds averaged Navier-Stokes (equations).

VOF Volume of fraction.

NOMENCLATURE

B	m	Breadth of inlet
C	$m^{1/2}/s$	Discharge coefficient
C_μ	-	Constant in the k-ε model
$\overline{F}$	N/m^3	External body forces
$g / \vec{g}$	m/s^2	Gravitational constant / Gravitational vector
H	m	Total head
h	m	Thickness of water jet at outlet
h_v	m	Velocity head
k_ε	m^2/ s^2	Turbulent kinetic energy
$\dot{m}$	$kg/(m^3 \cdot s)$	Mass transfer between phases
p	Pa	Static pressure
Q	m^3/s	Discharge
S_m	$kg/(m^3 \cdot s)$	Mass added to the continuous phase from the dispersed second phase
t	s	Time
v	m/s	Velocity of water jet at outlet
$\vec{v} / \tilde{\vec{v}} / v_i$	m/s	Velocity vector / Favre- averaged velocity vector / Component of velocity vector
x / x_p	m	Horizontal position of jet flow / Horizontal position of middle of jet flow
y	m	Vertical position of jet trajectory
z	m	Vertical distance
α	-	Volume fraction variable
ΔS	m	Vertical distance between the bottom of the flip bucket and downstream water surface level
$\sum h$	m	Sum of head losses
ε	m^2/ s^3	Turbulent dissipation rate
I	-	Unit tensor
θ_0, θ_s	Rad	Angle of inclination from the horizontal plane of the water jet at outlet
λ	-	Scale factor
μ / μ_t	kg/ (s·m)	Molecular viscosity / Turbulent eddy viscosity
$\rho / \overline{\rho}$	kg/ m^3	Density / Time averaged density
$\bar{\bar{\tau}} / \tilde{\bar{\tau}} / \tilde{\bar{\tau}}^R$	N/m^2	Viscous shear stress tensor / Favre-averaged viscous shear stress tensor / Reynolds stresses

TABLE OF CONTENTS

ABSTRACT

CFD is today a big part of the design process in hydraulic engineering and is more economical and time efficient than traditional scale models. But, there are still issues concerning the agreement with scale models in large and complex geometries.

In this degree project a high head, five channeled, slotted flip bucket spillway system is analyzed with the CFD software FLUENT and compared with existing scale model results. The sought hydraulic parameters in each channel were the discharge capacity, the pressure distribution and the throw distance from the flip buckets.

The discharge capacity and pressure distribution was practically equal for all five channels and only the throw distance from Channel 1 deviated from the others. The agreement with data from the scale model is quite low.

The biggest error sources behind the bad agreement may depend on the lack of computational power which led to bad choice of cell size, model delimitations and simplifications.

CFD models can easily be built up by people without experience in hydraulics which can lead to fatal errors when building up the model and interpreting results. Hence, long experience in CFD or verification of the numerical results with several different hydraulic parameters is the only way to guarantee qualitative results from CFD modeling.

Keywords: Computational fluid dynamics; FLUENT; VOF; Open channel flow; Slotted flip bucket spillway; Discharge capacity

1. INTRODUCTION

In the mid 1900's, computational fluid dynamics, popularly known as CFD, was introduced in the aircraft industry and is nowadays an obligatory part of its design process. CFD is today also a big part of research and design in many other areas, like: medicine, turbine optimization, engine construction and electrochemistry. (Hirsch, 2007)

Civil engineers have also begun to use CFD and the usage in hydraulic designs increase constantly. Nevertheless, scale modeling is still being used to confirm CFD results where complex hydraulic conditions occur and in cases where CFD modeling not yet has been validated. (Sassaman et al, 2009)

1.1. Objectives

In the present study, CFD modeling is used to investigate hydraulic characteristics in the high head Shibuya hydropower spillways and confirm experimental scale model data.

The discharge coefficients for each spillway and for all spillways together will be presented and the spillway with the highest discharge capacity will be determined. The discharge capacity from the numerical modeling will then be compared with the results from the scale model.

The static pressure distribution along the channels will be presented and in three of the five channels the numerical static pressure will be compared with pressures from the scale model.

The flip bucket throw distances will be calculated and the length of the span of the plunging jets will be determined for each channel using empirical equations.

1.2. Delimitation

When using CFD the computational power and memory resources are of greatest essence. In this study, a number of cases had to be modeled on a limited time and only laptops were available for the computations. Those

limitations restricted the practical maximum number of cells to a number too low for such an enormous structure.

The calculations of the flip bucket throw distances will be carried out using empirical equations instead of modeled by CFD. The interaction between the jet flow and the air is too complicated and computational expensive.

In the constructed spillway system, there are air inlets at several locations along the spillways. These inlets have been excluded in this study because they also were excluded in the scale model.

2. THEORETICAL BACKGROUND

This chapter will act as a theoretical foundation upon which the methods, results and discussion will be based. The first section will give a short introduction to the project investigated, the Shibuya Hydropower project. The next three sections present different modeling types: analytical and empirical modeling, scale models and CFD.

2.1. The Shibuya Hydropower Project

The Shibuya Hydropower Project, located in the Qingjiang River in the Hubei Province, China, was at time of construction the major power source for peak load regulation in the Central China Power Grid. It is an enormous project with a 233 meter high concrete faced rockfill dam (CFRD), the world's highest of this type at time of construction, a reservoir capacity of 4,58 billion cubic meters and a total spillway capacity of about 18 000[1] cubic meters per second (Zhang et al, 2008).

The project also consists of an underground power station and a curved, stair stepped approach channel which terminates in a five channel spillway system, see Figure 1. The five channels have identical geometry at the inlets and in the first parts of each channel. After about 180 meters the channels are slightly different designed with horizontal lengths varying from 230 to 300 meter and with elevation drops, from crests to

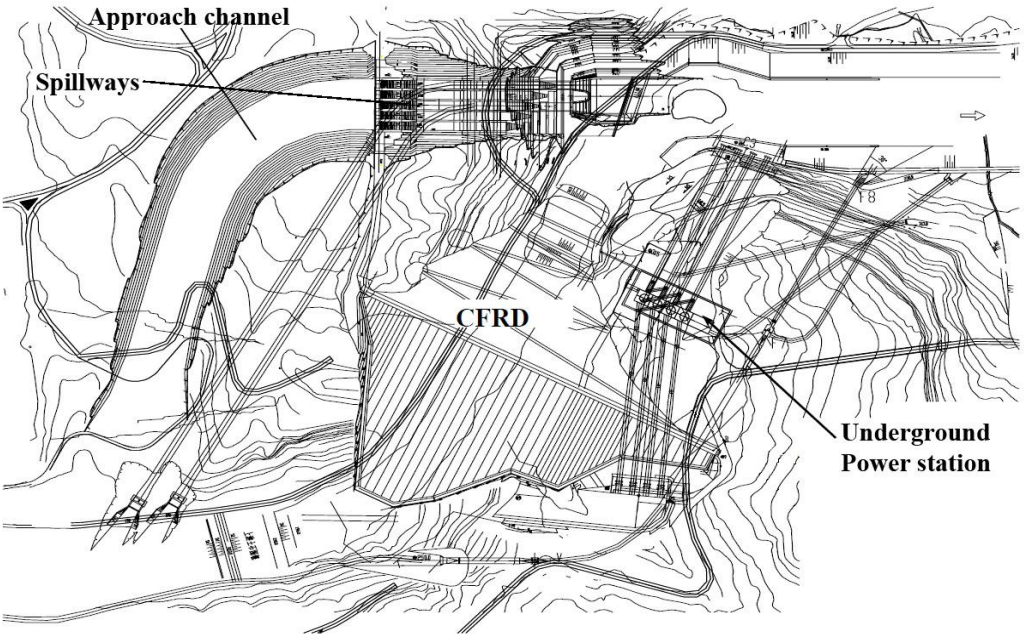

Figure 1. Plan view of the Shibuya Hydropower Project (Zhang et al, 2008)

[1] When all spillways discharge the design flood and the sluice tunnel is at maximum discharge.

the bottoms of the slotted flip bucket outlets, from 70-125 meter. For more information about the spillway layout, see Appendix A.

2.2. Analytical and empirical modeling

There are a variety of analytical and empirical models in hydraulics but they all have in common that they are only valid for a certain flow condition or geometry. In this study, analytical equations have been used for calculating the discharge capacity of the spillways and to determine a theoretical water depth close to the inflection point in the first linear part of the spillway channels to validate numerical and experimental results. Two empirical equations have been used to calculate the throw distance from the flip buckets.

2.2.1. *Discharge capacity of a rounded weir*

When determining the discharge capacity of a rounded weir, equation (1) from Häggström (2009) can be used.

$$Q = CBH^{3/2} \tag{1}$$

When determining the discharge coefficient for the spillway system in this study, B is defined as the sum of the crest lengths for all channels and C is an average discharge coefficient for the whole system.

2.2.2. *The energy equation*

For a simple approximation of the water depth in the channels, Bernoulli's equation (Häggström, 2009) can be used. The equation is derived from the conservation of energy and displays the relationships between potential and kinetic energy and pressure, eq. (2).

$$p + \rho g z + \frac{1}{2}\rho v^2 = const. \tag{2}$$

The equation is valid along a streamline, if the fluid has constant density, if the flow is steady and if energy losses are neglected. A more common form of eq. (2) in hydraulic applications is eq. (3), the energy equation.

$$z_1 + \frac{v_1^{\,2}}{2g} + \frac{p_1}{\rho g} = z_2 + \frac{v_2^{\,2}}{2g} + \frac{p_2}{\rho g} + \Sigma h \tag{3}$$

2.2.3. *Flip bucket throw distance*

Many different equations have been used for calculating the throw distance when designing flip bucket spillways. But most of the existing equations are only valid for certain conditions and geometries and are not applicable for high heads. Equation (4) from Wahl et. al (2008) and equation (5) from Li (2007) were though found to present reasonable results.

$$\frac{x}{h_v} = \sin 2\theta_0 + 2\cos\theta_0 \sqrt{\sin^2\theta_0 + \frac{y}{h_v}} \tag{4}$$

$$x_p = \frac{v^2 \sin\theta_S \cos\theta_S + v\cos\theta_S \sqrt{v^2 \sin^2\theta_S + 2g\left(\Delta S + h\cos\theta_S\right)}}{g} \tag{5}$$

2.3. Scale modeling

Dam overtopping is mentioned by Hanson & Temple (2007) as one of the most common causes of dam failure and is a consequence of when inflow exceeds the capacity of the reservoir and the spillway outflow

system. Therefore, when designing new spillways or evaluating the safety of existing ones e.g. according to higher design floods, determination of discharge capacity is of the essence.

Other hydraulic parameters such as water level, velocity profiles and pressure fields are also of big importance for the security of the structure. A change in the velocity profiles might induce scour at critical sections and a change in flow may lower the pressures so cavitation occur.

To obtain all hydraulic characteristics required for a new design or evaluating an existing one due to changes in design floods, a model of the structure has to be created. Complex hydraulic structures are hard to describe in an analytical way and are traditionally simulated in scale models. The results from scale models are often used in the design process and are usually of a high standard (Yang, 2006). Unfortunately scale models are expensive, both in aspect of time and money and errors due to scale effects may increase with growing ratio of prototype to model size (Kim & Park, 2005).

2.3.1. *Scale model experiments on the Shibuya spillways*

Scale model experiments on the Shibuya hydropower spillways have been carried out at the State Key Laboratory of Hydro Science and Hydraulic Engineering at Tsinghua University in Beijing, China. The experiment investigated three different spillway schemes with varying layout of the terminal structures. Since the scale model is a free surface model gravity is the main governing force implying that Froude's model law is used for the non geometrical parameters, Table 1. The parameters analyzed in the conducted experiment were the pressure distribution along the bottom of the spillway channels and the maximum equilibrium scour depth in the downstream river. One of the schemes investigated was chosen for the final design and a simplified version of that scheme was investigated in this study.

The results from the scale model included pressure distributions for three of the five channels for four different discharge rates, see Table 2. The highest of the discharge rates represents the 500-year flood. (Zhang et al, 2008)

Table 1. Scale factors according to Froude's model law (Zhang et al, 2008)

	Label	Relation to length scale	Scale
Length	λ_L	-	1:100
Time	λ_t	$\lambda_t = \lambda_L^{0.5}$	1:10
Velocity	λ_v	$\lambda_v = \lambda_L^{0.5}$	1:10
Discharge	λ_Q	$\lambda_Q = \lambda_L^{2.5}$	1:100 000

Table 2. Discharge rates and water levels represented in the scale model

Discharge rate	Flood frequency	Water level	
		Upstream	Downstream
7 240 m³/s	20.0 %	-	-
10 000 m³/s	5.0 %	-	-
11 940 m³/s	1.0 %	398.0 m	222.0 m
14 810 m³/s	0.2 %	400.8 m	226.8 m

2.4. CFD

Because of the rigid and expensive nature of scale models, more dynamic alternatives have been developed, numerical methods. Numerical modeling in hydraulics has grown bigger the recent years due to vast improvements in computing capacity and developments of commercial software. Numerical modeling is less expensive and more time efficient than scale modeling, but there are still issues concerning the accuracy of the results.

Numerical modeling in fluid flow is called CFD and is by Hirsch (2007) defined as "the set of methodologies that enable the computer to provide us with a numerical simulation of fluid flows [2]". A CFD simulation can be divided into three stages, namely: pre-processing, solving and post-processing. In the following sections the background of CFD and the three stages in a simulation will be explained.

2.4.1. *Background*

In the first half of the 1800's C. L. Navier, S. Poisson, J. C. Saint-Venant and G. Stokes came up with various forms of equations governing fluid

dynamics and in 1846 Stokes presented a short and simple derivation of the equations, thus the Navier-Stokes equations. The Navier-Stokes equations are a set of non-linear partial differential equations which governs the motion of a Newtonian fluid [3] in space and time. The equations describe the conservation of continuity, momentum and energy[4]. They are the only equations needed[5] for describing the motion of fluids and they are the foundation of modern CFD. (Hirsch, 2007)

According to Chung (2002) the modern computational fluid dynamics was born in the 1950's when the digital computers were introduced. The main issue when modeling and developing computational fluid dynamics has always been computational power. The first CFD calculations used a form of the Navier-Stokes momentum conservation equation where the viscosity and vorticity terms were excluded which resulted in potential equations. The potential equations describe fluid flow in a very simple way and cannot model turbulence (Hirsch, 2007).

Because most fluid flows in reality are turbulent, ability to model turbulence is a necessity in modern computational fluid dynamics. With increasing computational power, a parallel development of numerical algorithms took place and a variety of turbulence models with different levels of approximation were developed.

---

[2] The definition of a fluid flow is when a sufficiently high number of particles affects and dominates the motion of each individual particle. (Hirsch, 2007)

[3] A fluid is Newtonian if it satisfies certain physical demands. The characteristic that usually fails a fluid to be Newtonian is when the stress is not linearly related to the strain. Water and air are under normal conditions Newtonian fluids. (Drazin & Riley, 2006; Panton, 2005)

[4] There are different opinions about which conservation laws are part of the Navier-Stokes equations. Mathematical books tend to assign only the conservation of momentum to the Navier Stokes equations whilst hydro dynamic books tend to include the conservation of mass, momentum and energy. Since this is a hydraulic research, the authors will assume that the Navier-Stokes equations consist of all three conservation laws. (Drazin & Riley, 2006; Hirsch, 2007)

[5] Although the Navier-Stokes equations are the only equations needed for determination of a fluid motion one must also define viscosity and thermal conductivity relations and the nature of the fluid. (Hirsch, 2007)

Reynolds averaged Navier-Stokes (RANS) models are the oldest turbulence models and most widely used in the industry. They were developed by O. Reynolds in the late 1800's. The turbulent fluctuations in the Navier-Stokes equations are averaged in time which adds an extra term to the momentum conservation equation, the Reynolds stresses. One of the most used RANS models is the k-ε model (Poroseva & Iaccarino, 2001), which will be further explained in chapter 3.2.1 FLUENT.

Nowadays we are able to simulate the whole range of turbulent fluctuations using a scheme called Direct numerical simulation[6] (DNS) which solves the Navier-Stokes equations without any external turbulence model. Unfortunately there is not, and will not be, enough computer capacity in the near future to use DNS for industrial purposes. So the use of DNS today is restricted to research on turbulent behavior and for refining lower levels of turbulence approximation schemes. (Hirsch, 2007)

2.4.2. *Pre-processing*

The ultimate goal of pre-processing stage is to transform a real structure into a computable model. This involves: building up the geometry, discretize the geometry and assign boundary types to your model.

Geometries can in much pre-processing software be imported from CAD-programs like Auto-CAD or MicroStation. It can also usually be constructed in the pre-processing program itself. The most important thing in this part is to decide the extension of your model in space. A bad positioning of the boundaries can affect the results significantly.

Because CFD is a numerical method, the system treated has to be discretized into computable control volumes, cells. All cells create a mesh. A mesh can either be structured or unstructured. In 2D, structured and unstructured mesh are comprised by quadrilateral cells and triangles respectively, see Figure 2. An unstructured mesh, in 3D, is comprised by polyhedrals, usually tetrahedrals, and is easily generated with automatic mesh generators. A structured mesh is, in 3D, only comprised by hexahedrals and is very hard to create for advanced geometries with an automatic mesh generator.

The quality of the results from CFD simulations are highly dependent on mesh structure, especially when working with open channel flow, and

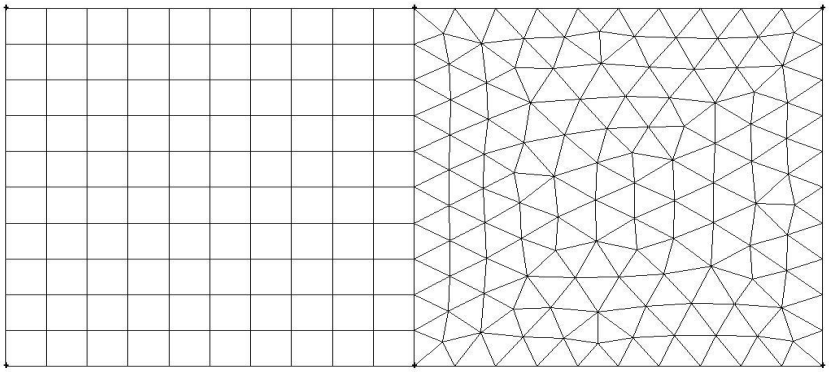

Figure 2. Structured and unstructured mesh in 2D

[6] Even though scientists believe that turbulence is governed by the Navier-Stokes equations it is not yet confirmed and the physical nature of turbulence is far from fully understood (Fefferman, 2006).

Margeirsson (2007) shows that structured mesh should be used whenever reasonable.

Another important aspect when building up a mesh is to create denser mesh where great velocity gradients occur, e.g. close to boundaries. With decreasing velocity gradients, a similar decrease in mesh density should be sought to minimize the total number of cells. (Hirsch, 2007)

When the geometry is constructed and the mesh is generated and approved, the first stage of the numerical simulation is finished. The next step is to export the created mesh into a solver, which will be explained in the next section.

2.4.3. *Solving*

In the solving phase a pre-defined mesh is imported into a numerical solver. After the required information is provided and the settings are chosen, the solver uses the Navier-Stokes equations to generate a numerical solution to the problem, see chapter 3.2.1 FLUENT for the governing equations.

When two or more phases need to be analyzed in the same model a multiphase model is required. One such model is the volume of fluid[7] VOF method proposed by Hirt & Nichols (1981). The VOF method is based on the assumption that two or more phases are not interpenetrating (FLUENT inc., 2006). All control volumes (cells) contain fractions from at least one of the phases and the sum of fractions in each control volume must add up to unity.

When a solution has been obtained, the next stage in the process is to present and validate the results.

2.4.4. *Post-processing*

When a solution is obtained from a numerical solver, the results must be interpreted and presented in a convenient way. Most commercial solvers have post-processing included in the software and the results may be presented instantaneous in the form of graphs, tables and animations.

If the solver has no function for post-processing or if the parameters sought cannot be obtained directly from the software one might have to process the data manually using text data outputs and external programs.

3. METHODS

The geometry construction and mesh generation in the pre-processing stage was made in the commercial software Gambit 2.3.16, which is the mesh and geometry generation program of FLUENT. For a complete description of the final geometry and mesh of the models in this study, see Appendix A.

ANSYS FLUENT 6.3.26 was used as solver and in parts of the post-processing. The other program used in the post-processing was Microsoft Excel.

3.1. Pre-processing

Turbulent fluid flow puts high demand on mesh density, especially in areas of high velocity gradients and in shear zones. In most complex 3D-cases the computational capacity, i.e. CPU, memory and disk space, limits the total number of cells and thus the accuracy of the solution declines. To keep the mesh density on a qualitative level, simplifications

[7] In FLUENT named the volume of fraction method

in geometry can be used. Therefore five different cases were evaluated to find out how different simplifications affected the results.

3.1.1. *Determination of final geometry and mesh*

As a result of the discussion above, five different models were created and modeled with the same settings to achieve a robust geometry and mesh density, see Table 3.

A model where all five channels and 400 meter of the approach channel was first modeled. The mesh in this model was very coarse and unstructured at the inlet due to the complex geometry. **Case 1**

Channel 1 alone was meshed including a 55 meter long and 19 meter wide strip of the approach channel. A series of simplifications were made, e.g. the inflow was assumed to be perpendicular to the inlet and therefore, symmetry about the longitude central plane could be used. Another approximation is the assumption that the flow is evenly distributed in all channels. When these conditions were set Channel 1 was meshed with three different mesh intensities, each with a successively increasing number of cells. **Case 2, 3 and 4.**

To check whether 55 meter is enough for the upstream water surface elevation to stabilize, a model with 150 meter of the approach channel was also created, **Case 5**.

All five cases were run and the pressure distributions in Case 1-4 were compared. The results can be viewed in Figure 3 and no obvious differences between the four models could be found. Based on the results in Figure 3 a decision to use separately modeled symmetry channels was made.

To better judge which case would be best fit for the project, another comparison was made. The difference in static pressure between Case 2 and 3, Case 2 and 4 and Case 3 and 4 for the 17 points were plotted in Figure 4. It can be seen that the difference between Case 3 and 4 is in general less than the others. This indicates that Case 3 and 4 are quite similar but different from Case 2. Because Case 4 has almost twice as many cells as Case 3 but generates almost the same result, Case 3 is chosen.

At last, a control if 55 meters of the approach channel is enough to achieve an unaffected upstream water surface elevation was performed. In Figure 5the reader can see that the water surface is stabilizing around 90 meters before the crest. Unfortunately there is only 55 meters of

Table 3. Model description of the four cases which will aid the choice of geometry and mesh

Case	Model description	Number of cells
1	All five channels plus 400 meters of the approach channel, very course mesh, no boundary layers	185 767
2	Channel 1 plus 55 meter of the approach channel, symmetry, course mesh, no boundary layers	15 208
3	Channel 1 plus 55 meter of the approach channel, symmetry, medium mesh, medium boundary layers	145 794
4	Channel 1 plus 55 meter of the approach channel, symmetry, fine mesh, fine boundary layers	258 921
5	Channel 1 plus 150 meter of the approach channel, symmetry, medium mesh, medium boundary layers	205 557

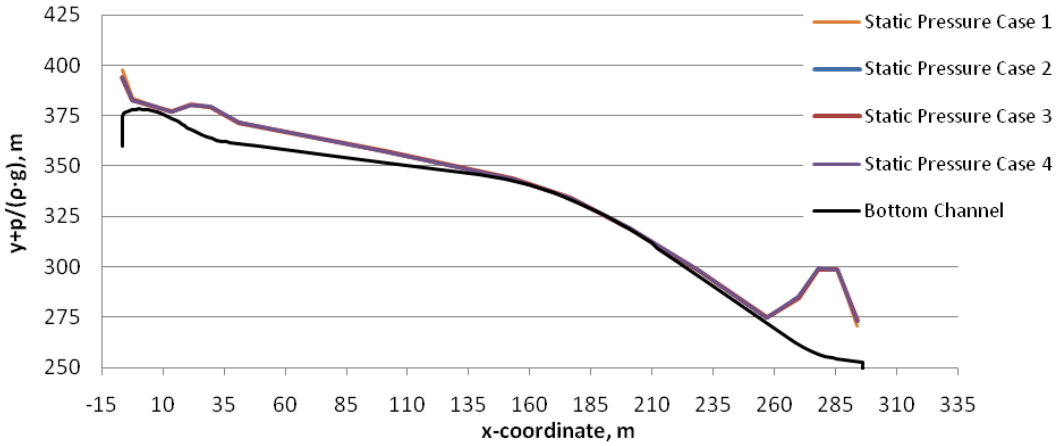

Figure 3. The static pressure distribution in Channel 1 for Case 1-4

straight channel before the crest (see plan view of the model in Appendix A) but there is only an elevation change of 5 centimeters from -55 meter to -150 meter.

Therefore, a 55 meter approach channel will be sufficient to obtain the "unaffected" upstream water level.

3.1.2. *Final geometry and mesh*

Case 3 was selected for the final geometry and five models, one for each channel, were created. Each model was constructed with a vertical symmetry plane along the longitude center of the channel. Fifty-five meters was proved to be enough length of the approach channel and the medium density mesh was chosen, which implicates a total cell number of about 150 000 cells per model.

When generating the mesh, boundary layers along the walls were used to minimize numerical errors. The cell size perpendicular to the walls and the bottom were made 0.2 meter with a growth factor of 1.26 until the full size was reached. The cell sizes differ in the model but the typical cell size in the spillway channels is 0.5 meter in vertical direction and 2 meters in the transversal and the longitudinal direction. See Figure 6 for a typical mesh layout.

After creating geometries and mesh, the boundary types were defined, see Figure 7 and Table 4. All faces surrounded by the model have been assigned to the boundary type Interior. The settings for each boundary were defined in the solver, which will be explained in the next section.

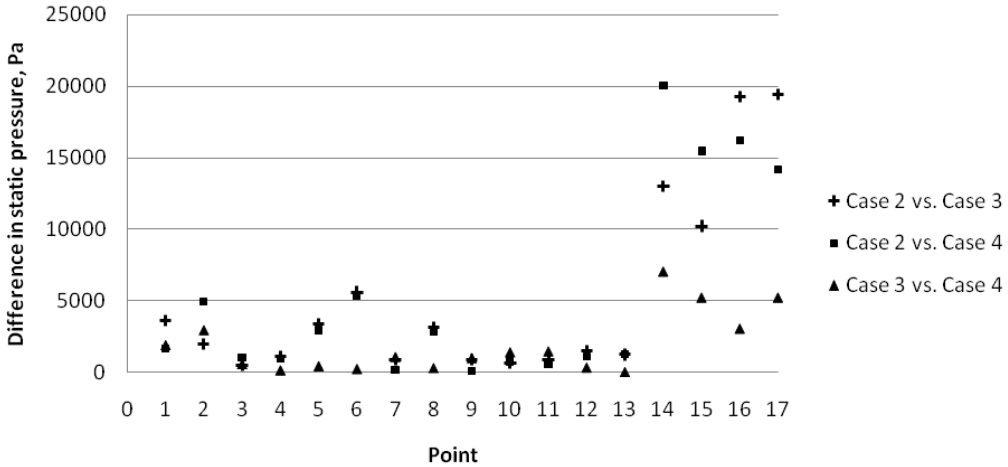

Figure 4. Differences between the static pressures for Case 2, 3 and 4

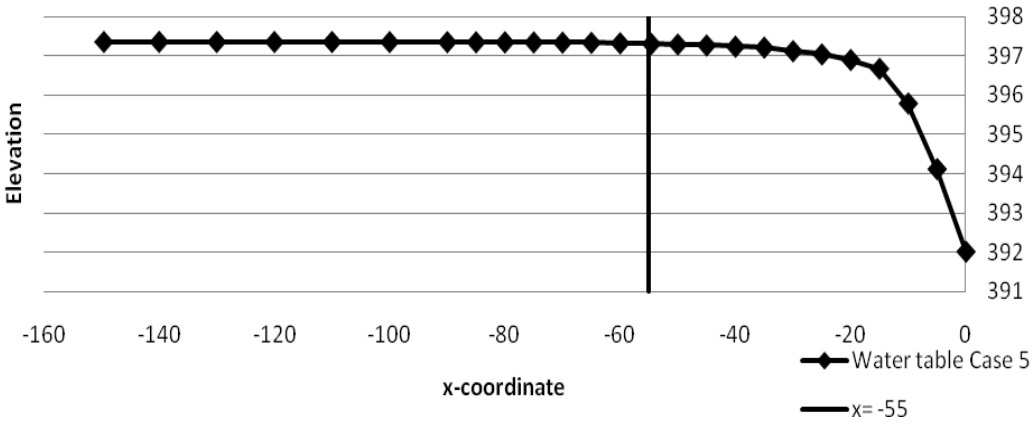

Figure 5. Water table in Case 5. The vertical line indicates where the inlets for Case 2-4 are

3.2. **Solving**

In the solving stage, the geometry and mesh were imported into FLUENT where all calculation took place. The software will be presented further in the first part of the Solving section and all information presented is from FLUENT inc. (2006).

In the next section, the settings used in FLUENT for this study will be shown. Settings not mentioned in the text are kept as default. The chosen settings are a result from following the recommendations by FLUENT inc. (2006) and experience gained during the study. All graphical user interface menus and choices in FLUENT will be typed in **bold**.

3.2.1. ***FLUENT***

FLUENT is a commercial CFD software in the ANSYS incorporation. FLUENT uses a Finite volume method (FVM) to solve the Navier-Stokes equations. FLUENT solves the conservation equations for mass and momentum in all applications but the energy conservation equations is optional depending on the type of simulation. In eq. (6) and eq. (7) the

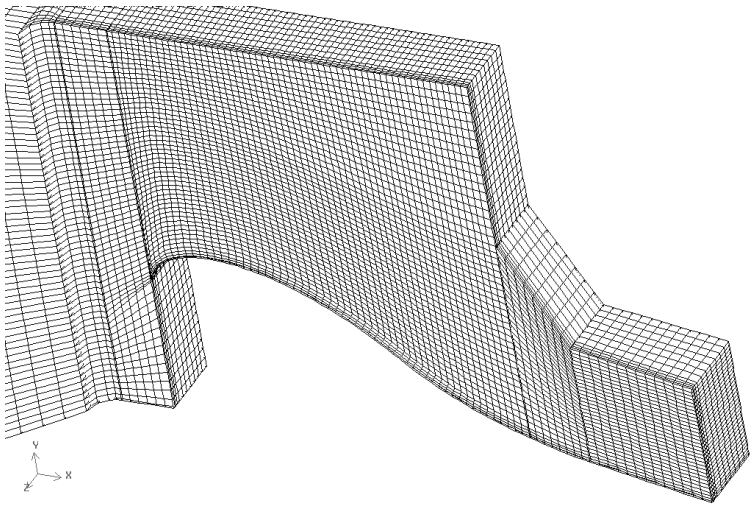

Figure 6. Cut through a typical section of one of the five symmetry channels. Near the bottom and the outer wall one can see that the mesh is denser, which is the boundary layers

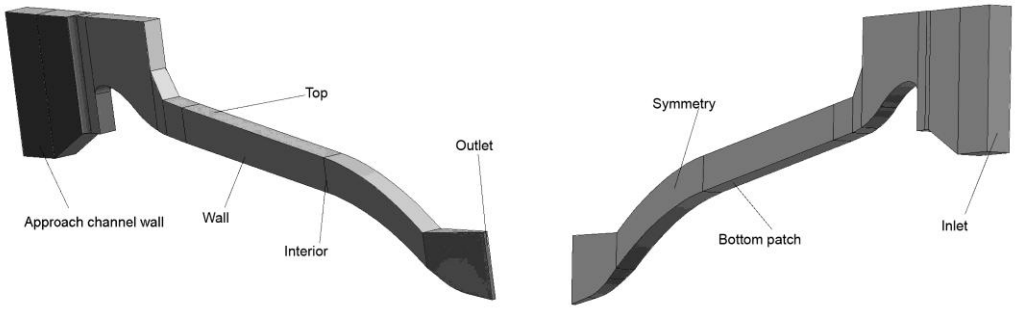

Figure 7. Schematic figure showing boundary names

conservation equations for mass and momentum in laminar flow, in a non accelerating reference frame are described.

$$\frac{\partial \rho}{\partial t} + \nabla \cdot (\rho \vec{v}) = S_m \tag{6}$$

$$\frac{\partial}{\partial t}(\rho \vec{v}) + \nabla \cdot (\rho \vec{v} \vec{v}) = -\nabla p + \nabla(\bar{\bar{\tau}}) + \rho \vec{g} + \vec{F} \tag{7}$$

Where the stress tensor $\bar{\bar{\tau}}$ is defined by eq. (8).

$$\bar{\bar{\tau}} = \mu\left[\left(\nabla \vec{v} + \nabla \vec{v}^T\right) - \frac{2}{3}\nabla \vec{v} I\right] \tag{8}$$

When the VOF-method is used to treat multiphase-phase models, the mass conservation equation (6) will get a slightly different look, the momentum conservation equation (7) will remain the same because of the dependence on the volume of fraction of the variables ϱ and μ. Eq. (9) show the mass conservation equation adjusted to the VOF-method.

$$\frac{1}{\rho_q}\left[\frac{\partial}{\partial t}(\alpha_q \rho_q) + \nabla \cdot (\alpha_q \rho_q \vec{v}_q) = S_{\alpha_q} + \sum_{p=1}^{n}\left(\dot{m}_{pq} - \dot{m}_{qp}\right)\right] \tag{9}$$

Where a_q is the volume fraction of the qth phase. Equation (9) is not solved for the primary phase, only for the secondary phase (and the rest of the phases if there are more than two). Instead, FLUENT is using the connection defined by eq. (10).

$$\sum_{q=1}^{n} \alpha_q = 1 \tag{10}$$

Table 4. Boundary names and types

Boundary name	Boundary type
Bottom patch	Wall
Approach channel wall	Wall
Inlet	Mass-flow inlet
Interior	Interior
Outlet	Pressure outlet
Symmetry	Symmetry
Top	Pressure inlet
Wall	Wall

When a turbulence model is used, one or more equations are introduced. In this study the RANS model k-ε is used. When using a RANS turbulence model, an extra term is introduced in the momentum conservation equation by the time averaging process, eq. (11). The extra term is called Reynolds stresses and represents the effects from turbulence.

$$\frac{\partial}{\partial t}\left(\overline{\rho}\overline{\vec{v}}\right)+\nabla\cdot\left(\overline{\rho}\overline{\vec{v}}\overline{\vec{v}}\right)=-\nabla\overline{p}+\nabla\left(\overline{\overline{\tau}}\right)+\nabla\left(\overline{\overline{\tau}}^{R}\right)+\overline{\rho}\overline{\vec{g}}+\overline{\vec{F}} \tag{11}$$

The k-ε model relates the mean velocity gradients to the Reynolds stresses, this approach is called the Boussinesq approximation, eq. (12).

The turbulent eddy viscosity depends on the turbulent kinetic energy, kε and its dissipation rate, ε eq. (13)

$$\overline{\overline{\tau}}^{R}=\mu_t\left(\frac{\partial v_i}{\partial x_j}+\frac{\partial v_j}{\partial x_i}\right)-\frac{2}{3}\left(\rho k_\varepsilon+\mu_t\frac{\partial v_k}{\partial x_k}\right)\delta_{ij} \tag{12}$$

$$\mu_t=\rho C_\mu\frac{k_\varepsilon^{\,2}}{\varepsilon} \tag{13}$$

3.2.2. *Settings in FLUENT*

Since the energy forces were small compared with the other forces in the models, and temperatures were not of interest for this study, the **energy equation** was disabled.

When defining the **operating conditions**, the **operating pressure** was kept as default (atmospheric pressure) and the **reference pressure location** were located, as advised by FLUENT inc. (2006), where the second phase (water) never would exist during the solving, at the top of the inlet. **Gravity** and **specified operating density** was enabled where the latter were kept as default i.e. the density of the primary phase (air).

The **multiphase model** was chosen as the **volume of fraction** (VOF), the **VOF-scheme** is **implicit** and **open channel flow** and **implicit body force** was enabled. The two **phases** in the VOF-model were air and water, defined as primary and secondary phase respectively according to the guidelines provided by FLUENT inc. (2006).

The **viscous model** was chosen to be the **standard k-ε model** which is one of the most used turbulence models in the industry (Poroseva & Iaccarino, 2001).

In five of the six numerical models, the five channels are simulated separately and are using symmetry. This reduces the discharge rate in each channel to a tenth of the total discharge rate, see Table 5. The error due to the assumption that all channels discharge the same amount of water is according to Zhang (2010) of minor importance.

Table 5. Discharge in symmetry channels at evenly distributed flow

Discharge in full model	Discharge in symmetry channels
7 240 m³/s	724 m³/s
10 000 m³/s	1 000 m³/s
11 940 m³/s	1 194 m³/s
14 810 m³/s	1 481 m³/s

The boundaries created in Gambit were assigned **boundary conditions** in FLUENT, see Table 6. For the boundary conditions at the inlet during various discharge rates, see Table 7. For a more realistic modeling of the "Approach channel wall" the **shear condition** was changed from no-slip to specified shear with the value of zero and with a **roughness height** of 0 meter.

The **pressure-velocity coupling** was set to **SIMPLE**, the **pressure discretization** was set to **PRESTO!** and the **volume fraction discretization** as **Modified HRIC**. Due to lack of computational power, only first order discretizations were used for the other discretization parameters.

3.2.3. *Convergence*

As always with numerical processes, it is important to keep in mind that the solution depends on an iterative process and the results are approximations and no absolute values. In this study, a solution was considered converged when three convergence criteria were fulfilled, namely: the residuals were below a pre-defined **absolute criteria** (10^{-3}) and had stagnated, when the results from a surface monitor showing static pressure in the end of the channel had stabilized and when the flux report showed less than 0.2%[8] of flux imbalance. See Figure 8 for examples of convergence in residuals and a surface monitor.

3.3. Post-processing

When all models were simulated in FLUENT the interpretation phase started. The following sections explain how the sought results were found.

3.3.1. *Discharge capacity*

To determine the discharge capacity of the channels the discharge coefficient was sought. As can be seen in equation (1), the discharge coefficient is a function of the discharge and the total head.

Table 6. Settings of boundary conditions deviating from default values

Boundary name	Boundary Condition	Phase	Settings
Bottom patch	Wall	Mixture	Roughness height = 0.003 m
Approach channel wall	Wall	Mixture	Shear condition = Specified Shear Shear stress = 0,0,0 Pa Roughness height = 0 m
Inlet	Mass Flow Inlet	Mixture	Open channel Free surface level = * m Bottom level = 350 m
		Primary phase (air)	Mass flow-rate = * kg/s
		Secondary phase (water)	Mass flow-rate = * kg/s
Interior	Interior	-	-
Outlet	Pressure Outlet	-	-
Symmetry	Symmetry	-	-
Top	Pressure Inlet	-	-
Wall	Wall	Mixture	Roughness height = 0.003 m

*The settings will vary depending on the discharge rate, see Table 7.

[8] Convergence criteria recommended by FLUENT inc. (2006)

Table 7. Settings of boundary conditions at the inlet for all discharge rates

		Q= 724 m³/s	Q= 1 000 m³/s	Q= 1 194 m³/s	Q= 1 481 m³/s
Inlet	Free surface level	392.6 m	395.8 m	398 m	400.8 m
	Mass flow-rate air	458 kg/s	353 kg/s	265 kg/s	131 kg/s
	Mass flow-rate water	722 552 kg/s	998 000 kg/s	1 191 612 kg/s	1 478 038 kg/s

The discharge rate is already given as a boundary condition but the total head has to be evaluated.

When using the VOF-model there exists no absolute surface of the water. Instead, there is a region where the volume fraction of water in each cell gradually decreases from 1 to 0. The thickness of this region is highly dependent on the mesh intensity but due to the limitation concerning the maximum cell number, the water surfaces in the models were diffuse, see Figure 9a.

To aid the choice of volume fraction which may represent the surface, a verification model was created with a very dense vertical mesh around the expected surface elevation for the discharge rate 11 940 cubic meters per second, see Figure 9b.

In the latter model the water surface was assumed to exist at the elevation where the volume fraction was 0.5. This was considered as the "true" surface elevation. Then a comparison with the standard model was made and the volume fraction which had a surface elevation which matched the "true" elevation the best was chosen as the surface governing volume fraction.

3.3.2. *Pressure distribution*

The static pressure distribution along the spillway channels was determined in seventeen points (sixteen in Channel 5), where the first point was positioned a few meters before the spillway crest and the last one just before the spillway outlet. The x-coordinates for the points in Channel 1, 3, and 5 were provided by the experimental data from the scale model and the position of the points in Channel 2 and 4 were chosen at similar coordinates. See Appendix A for coordinates of the points. In FLUENT the static pressures were obtained by the function **XY Plot**. The results were by the function **XY Plot** exported to text files and post-processed in Microsoft Excel.

3.3.3. *Flip bucket throw distance*

In order to find the flip bucket throw distance of the jet flow at the channel outlets using equation (4) and (5), a few parameters has to be found: the water velocity profile at the outlet, the angle between the flow

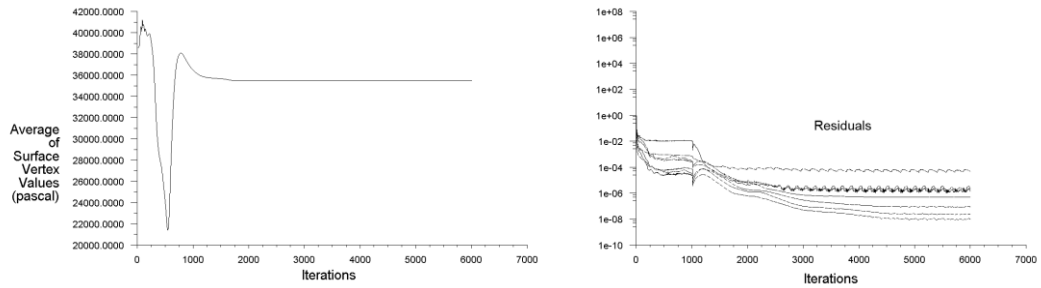

Figure 8. Examples of convergence in residuals and a surface monitor. Convergence in the surface monitor in this example is reached after about 3 000 iterations and in the residuals after about 5 000 iterations

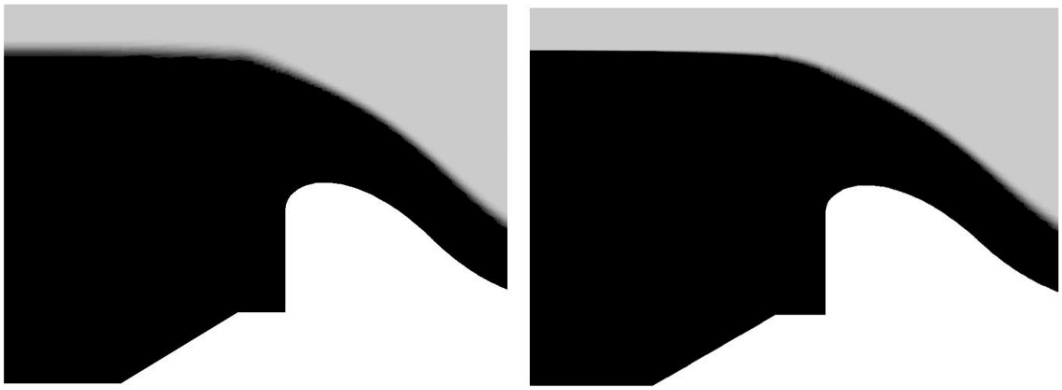

Figure 9. a) Diffuse water surface at inlet due to normal mesh density. b) Distinct water surface at inlet due to denser mesh about predicted surface elevation

direction and the horizontal plane and the distance from the bottom of the outlet to the downstream water table.

It is not possible to get the velocity profile of the water from pre-defined functions in FLUENT, only the mixed fluid, so to be able to get the velocity for the water at the outlet, a **custom field function** was created. The custom field function was created by multiplying the volume fraction of the water phase with the velocity magnitude of both the water and the air. This function will not generate accurate velocities around the surface where the VOF of water is less than 1 but that is taken into consideration.

Using the custom field function, the velocity profile at the outlet was obtained. The angle from the horizontal plane to the velocity vectors were measured by hand on vector plots. The elevation of the downstream water surface was obtained from Zhang et al (2008).

The throw distance was calculated with equation (4) at three heights per outlet: just above the spillway bottom, just below the water surface and where the velocity profile had its maximum. The span of the plunging water was then defined as the distance between the minimum and the maximum values of the throw distances. The calculations of throwing distance mentioned above are calculated for the flood rate 14 810 m^3/s for every one of the five spillway channels.

As a way to validate the results from equation (4) and for making a parametric study, the throw distances was also calculated with equation (5). In the parametric study the throw distances were calculated for all five channels and four discharge rates, see chapter 4.4 Results – Parametric study.

3.4. Validation of numerical model

Along with the comparison with scale model data, the energy equation was used to obtain an approximate value of the analytical pressure at the inflection point in the first linear part of the spillways. Another validation was a sensitivity test of the settings in the solver.

3.4.1. *Analytical determination of pressure*

An approximation to the pressure at the inflection point, see Figure 10, can be found by using the energy equation. By definition, the inflection point is where the stream lines are parallel with the bottom and therefore hydrostatic pressure occurs. If the flow in the channel is assumed to be

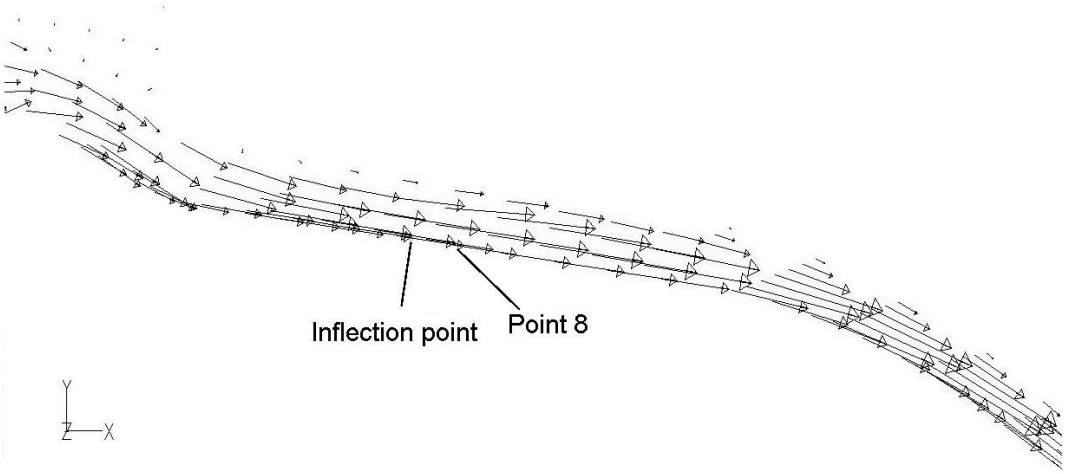

Figure 10. Vector plot of the first straight part of the channels

uniform[9] an approximation of the water depth can be calculated and thus the hydrostatic pressure can be estimated. The static pressure before the inflection point should be higher than the hydrostatic due to the momentum of the flowing water and less than the hydrostatic pressure after the inflection point.

The energy equation is applied from a section where the upstream water level is unaffected to point 8 (close to the inflection point). The water depth and the hydrostatic pressure then can be calculated.

3.4.2. *Sensitivity test of settings in numerical model*

As a way to verify and validate the results from the numerical simulations, eight modified runs with different settings were conducted for Channel 1 at the discharge rate 11 940 m^3/s, see Table 8 for an overview of the eight modifications.

The first control investigated whether an unsteady (time dependent) simulation would generate a different result. The time steps varied in a range from 10^{-6} to 1 second. **Modification 1**

Next some modifications of the inlet boundary conditions were made. Instead of using the default values for the kinetic energy and the turbulent dissipation rate, a hydraulic diameter of 32 meter and a turbulent intensity of 10 % were used. **Modification 2**

As a third validation, a series of modifications were done. The pressure discretization was set to body force weighted, the pressure-velocity coupling to fractional step and in the boundary condition for the outlet, backflow volume fraction for water was changed to 1. The model was then simulated in an unsteady mode where non-iterative time advancement was chosen in Transient controls. The time steps were as low as 10^{-6}. The settings in this modification are similar to the settings used by Halldén (2010), which generated good agreement with scale model results. **Modification 3**

The discretization scheme for momentum, turbulent kinetic energy and turbulent dissipation rate was changed from first order to second order. **Modification 4**

As a sensitivity test of the location of the pressure points in the z-direction, the points where the pressure were measured was moved

[9] In this sense, uniform means that the streamlines are parallel in the horizontal plane, i.e. no occurrence of cross waves etc. in the channels.

Table 8. Overview of the eight validation models

	Description of the modification
Modification 1	Unsteady solver
Modification 2	Change in boundary conditions at inlet
Modification 3	Unsteady solver, non-iterative time advancement, change in boundary conditions, change in pressure discretization scheme and change in pressur-velocity couplin
Modification 4	Change of discretization scheme for momentum, turbulent kinetic energy and turbulent dissipation rate from first to second order
Modification 5	Movement of all measuring points in the z-direction
Modification 6	Change of turbulence model to k-ω
Modification 7	Change of turbulence model to LES
Modification 8	Change of turbulence model to DES

0.5 meter away from the symmetry line. This was made in order to find out if any of the pressure measuring points in the scale model slightly deviated from the center. **Modification 5**

At last, three runs with different turbulence models were run. First the k-ω model was used, **Modification 6**.

This was followed by **Modification 7** where a LES model was used and **Modification 8** where a DES model was used. The k-ω model was run in a steady mode, but the LES and DES models were modeled in an unsteady mode.

As a way to control the correctness of the assumption that a fifth of the total discharge goes through one channel, a flux report will be generated at the spillway crests in the model with the five channels altogether.

4. RESULTS

4.1. Discharge capacity

The channel with the highest discharge capacity was sought in this study and the individual discharge coefficients for the five channels with fully open gates can be seen in Table 9. The discharge rate used in the calculations is one fifth of the total discharge rate. The way the boundaries have been chosen in this study assembly the flow conditions in a case where all five spillways are in use simultaneously.

The results at discharge from five spillways are shown in Table 10.

The results from the scale model experiments are limited in this parameter. There are only data on the unaffected upstream water level from two discharge rates available, see Table 11.

In Figure 11 and 12 both the numerical and the scale model results for the whole system are presented in the same graphs.

Table 9. Head and discharge coefficients for the five channels, at four different discharge rates, from the numerical modeling

	1 448 m³/s		2 000 m³/s		2 388 m³/s		2 962 m³/s	
	H	C	H	C	H	C	H	C
Channel 1	14,13	1,95	17,38	1,97	19,46	1,99	22,31	2,01
Channel 2	14,13	1,95	17,38	1,97	19,46	1,99	22,31	2,01
Channel 3	14,12	1,95	17,37	1,97	19,45	1,99	22,30	2,01
Channel 4	14,13	1,95	17,38	1,97	19,46	1,99	22,31	2,01
Channel 5	14,14	1,95	17,39	1,97	19,48	1,98	22,33	2,01

Table 10. The discharge coefficients for the five channels modeled together, at four different discharge rates, from the numerical modeling

	7 240 m³/s		10 000 m³/s		11 940 m³/s		14 810 m³/s	
	H	C	H	c	H	C	H	C
All channels	14,75	1,83	18,12	1,853	20,01	1,91	22,53	1,98

The largest deviation in discharge coefficient from the scale model is at the discharge rate 11 940 cubic meters per second and is 1.57 percent.

4.2. Pressure distribution

The pressure distribution for all five channels were determined numerically for the four discharge rates and compared with the available scale model pressures. The scale model results did not cover all of the channels so the numerical results for Channel 2 and 4 are only presented and not compared with the scale model values. The pressure distributions in the channels for the discharge rate 11 940 cubic meters per second are shown in Figure 13. In the figures, pressure results from three different configurations can be seen: numerical simulation of each channel separately, numerical simulation of all channels at the same time and the results from the scale model. A comparison between the pressures from the scale model and the separately modeled channels can be seen in Table 12 and 13.

All pressure distributions of the investigated discharge rates and channels can be viewed in Appendix B.

4.3. Flip bucket throw distance

After computing the throw distances, the maximum value and the minimum value for the discharge rate 14 810 cubic meters per second were compared to get the span. The results can be seen in Figure 14 and Table 14.

4.4. Parametric study

In this section the effects of changing one of the key variables will be investigated. This procedure is performed in order to investigate how varying conditions tend to affect the results.

First the effects from a varying discharge rate on several results will be investigated and then the effects from changes in channel length will be looked into.

Table 11. The discharge coefficients for the spillway system, at two different discharge rates, from the scale model experiment

	11 940 m³/s		14 810 m³/s	
	H	C	H	C
All channels	19,8	1,94	22,6	1,97

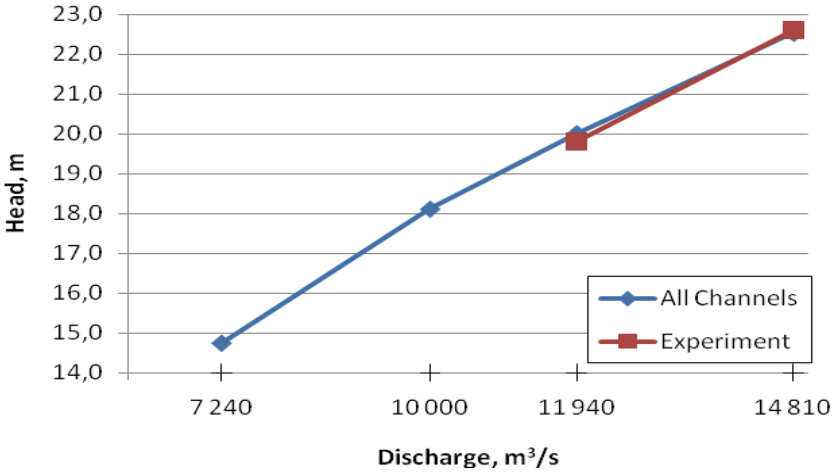

Figure 11. Head as a function of discharge rate for the spillway system

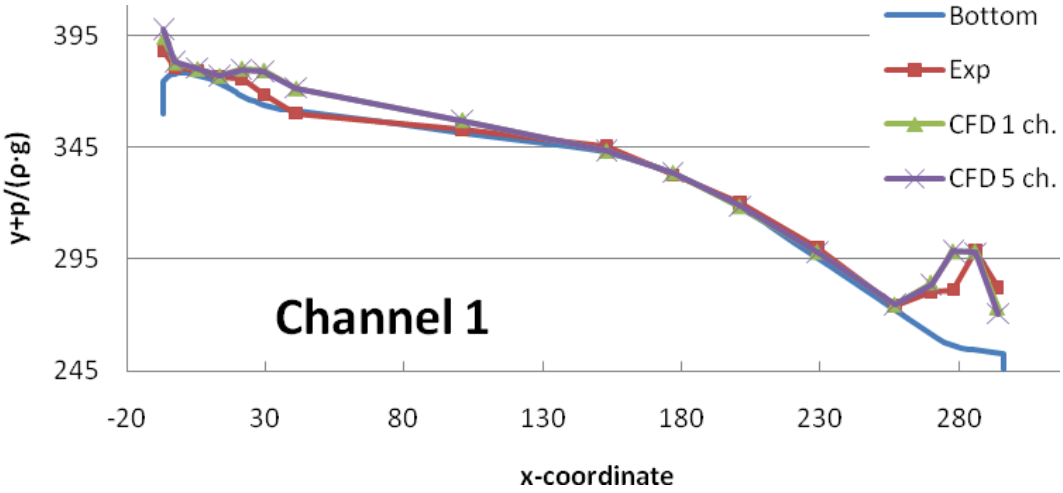

Figure 13a. Numerical and scale model (Exp.) pressure distributions at the discharge rate 11 940 m³/s, Channel 1

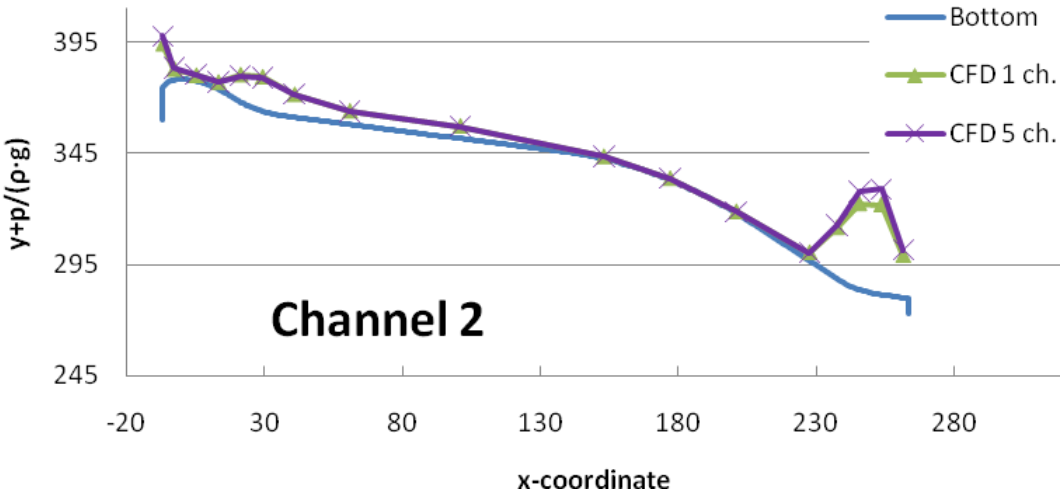

Figure 13b. Numerical and scale model (Exp.) pressure distributions at the discharge rate 11 940 m³/s, Channel 2

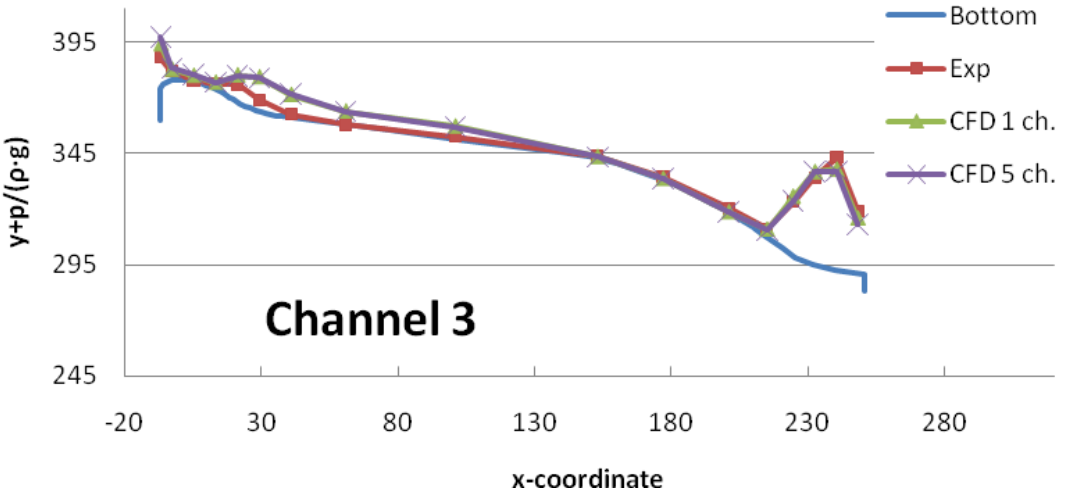

Figure 13c. Numerical and scale model (Exp.) pressure distributions at the discharge rate 11 940 m³/s, Channel 3

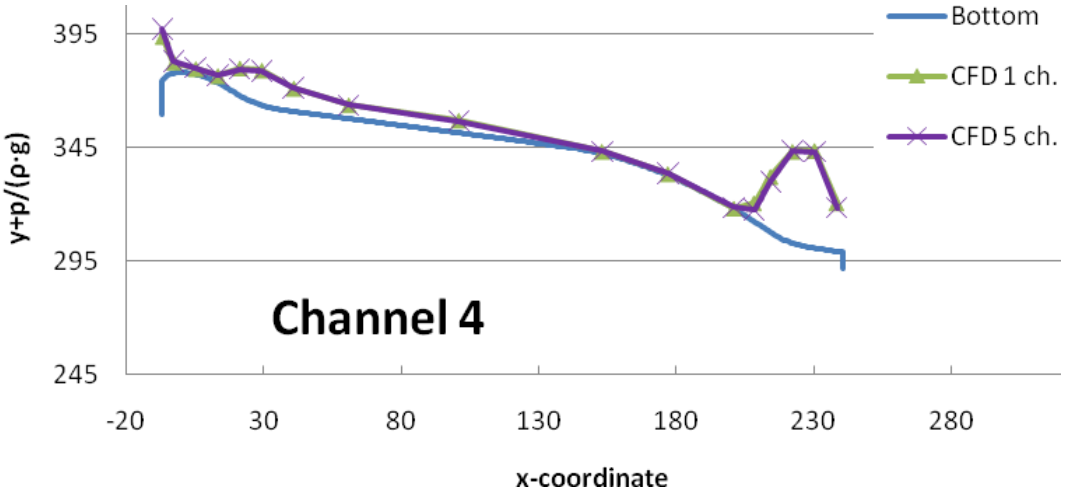

Figure 13d. Numerical and scale model (Exp.) pressure distributions at the discharge rate 11 940 m³/s, Channel 4

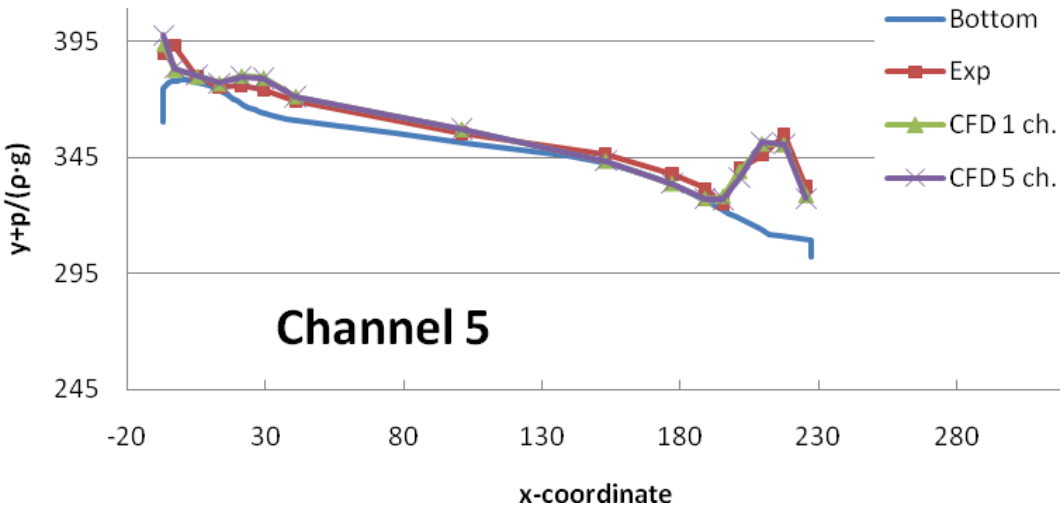

Figure 13e. Numerical and scale model (Exp.) pressure distributions at the discharge rate 11 940 m³/s, Channel 5

Table 12. Pressures from the separately modeled channels (p_{CFD}) and the scale model (p_{exp}) at discharge rate 11 940 m³/s. Channel 5 has only 16 measuring points

Point	Channel 1		Channel 2	Channel 3		Channel 4	Channel 5	
	p_{CFD} (kPa)	p_{exp} (kPa)	p_{CFD} (kPa)	p_{CFD} (kPa)	p_{exp} (kPa)	p_{CFD} (kPa)	p_{CFD} (kPa)	p_{exp} (kPa)
1	194	135	194	194	134	194	192	148
2	49	26	49	48	39	49	48	148
3	25	18	25	25	5	25	25	23
4	30	28	30	30	24	30	30	15
5	119	74	120	120	78	120	119	77
6	152	47	152	152	52	152	153	101
7	100	-8	101	101	15	101	101	77
8	54	13	60	60	0	60	55	36
9	9	30	55	55	10	55	10	40
10	6	-4	10	10	12	10	8	48
11	5	21	7	7	16	7	10	53
12	29	48	6	6	22	3	61	26
13	27	20	36	38	40	81	210	223
14	230	186	230	262	236	244	373	321
15	414	241	382	417	389	400	393	430
16	436	438	399	451	499	426	190	224
17	201	288	188	247	278	211	-	-

Table 13. Comparison between numerical pressures and scale model pressures

Point	Channel 1		Channel 3		Channel 5	
	$p_{CFD} - p_{exp}$ (kPa)	$\Delta p / p_{exp}$ (-)	$p_{CFD} - p_{exp}$ (kPa)	$\Delta p / p_{exp}$ (-)	$p_{CFD} - p_{exp}$ (kPa)	$\Delta p / p_{exp}$ (-)
1	59	*44%*	60	*44%*	44	*30%*
2	23	*87%*	9	*24%*	-99	*-67%*
3	7	*37%*	20	*411%*	3	*11%*
4	2	*9%*	6	*25%*	15	*96%*
5	45	*61%*	41	*53%*	43	*56%*
6	105	*224%*	100	*193%*	51	*51%*
7	108	*	86	*559%*	24	*31%*
8	41	*306%*	59	**	19	*51%*
9	-21	*-69%*	44	*424%*	-30	*-75%*
10	10	*	-2	*-15%*	-40	*-84%*
11	-17	*-78%*	-9	*-54%*	-43	*-81%*
12	-19	*-40%*	-16	*-73%*	36	*137%*
13	7	*35%*	-3	*-7%*	-12	*-6%*
14	44	*23%*	26	*11%*	52	*16%*
15	172	*71%*	28	*7%*	-37	*-9%*
16	-1	*0%*	-49	*-10%*	-33	*-15%*
17	-87	*-30%*	-31	*-11%*	-	-

* The scale model pressures are negative and therefore no percental comparison can be done.

** Due to low scale model results a percental comparison generated numbers with no real significance.

Table 14. Flip bucket throw distances for the discharge rate 14 810 m3/s

	Min. throw length eq. 4	Max. throw length eq. 4	Span	Throw length eq. 5
Channel 1	73	168	95	121
Channel 2	87	177	90	148
Channel 3	113	184	71	157
Channel 4	111	188	77	160
Channel 5	113	182	69	161

4.4.1. *Effects from change in discharge rate*

The effect from change in discharge rate on the discharge coefficient (Figure 15), the head (Figure 16), the pressure distribution (Figure 17), the maximum velocity at the outlet (Figure 18) and the throw distance (Figure 19) will be presented in this section.

4.4.2. *Effects from change in channel length*

In this section the effects from change in channel length on pressure distribution and discharge capacity will be investigated. In Figure 20, 21 and 22 the static pressure distribution up to the point where the geometry of the five channels starts to diverge, about x = 180 meter, is presented.

4.5. Results from validation of numerical model

This section presents the results from the two extra validation controls that were performed. First, the analytical pressure at the inflection point will be presented. Secondly, the results from the sensitivity test are presented.

4.5.1. *Analytical determination of pressure*

The analytical pressure at the inflection point was calculated without considering the head losses due to bed friction and losses at the entrances to the channels. In Figure 23 the numerical pressure distribution, the pressure distribution from the scale model and the analytical pressure at the inflection point is plotted. For calculations of the analytical pressure, see Appendix C.

4.5.2. *Validation of settings in numerical model*

The pressures from the validation controls and the final results were compared to the scale model data in Channel 1, see Table 15. **Standard**

represents the settings used when evaluating model geometry, discretization and for the final results.

Mod. 7 and Mod. 8, LES and DES configurations respectively, had problems to converge. Hence, these simulations did not give a result that could be used as a validation control.

In the flux reports from the model with the five channels modeled together it can be seen that the maximum difference between the individual discharge rates for the five channels were 1.1 percent.

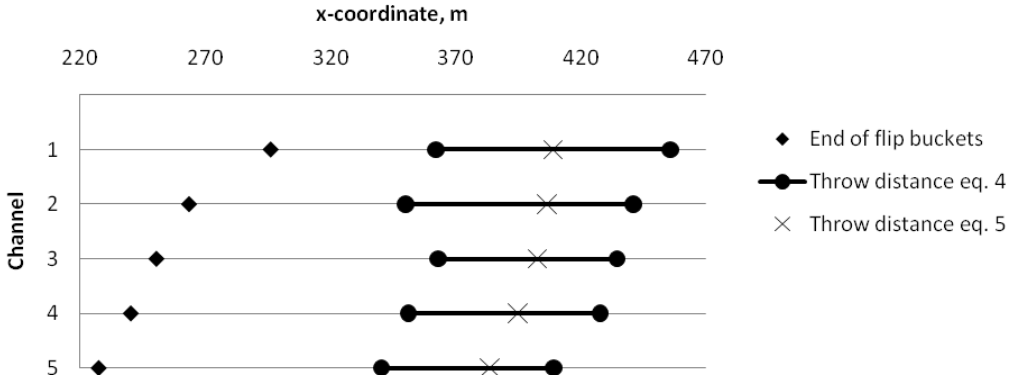

Figure 14. Flip bucket throw distances when the discharge rate is 14 810 m3/s

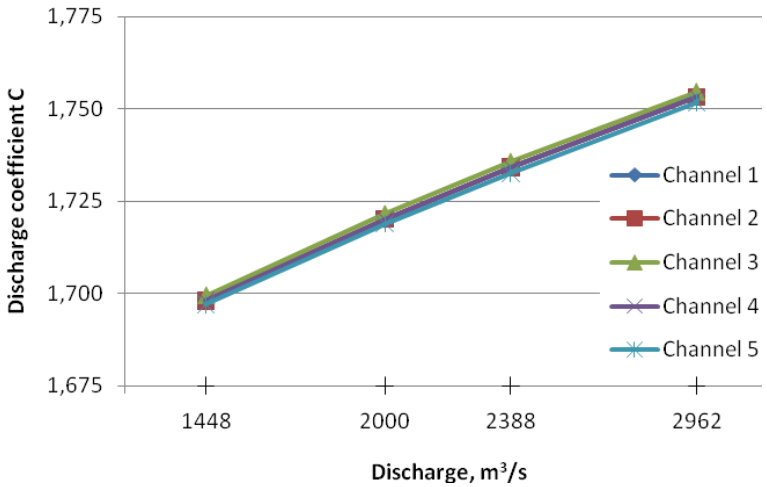

Figure 15. Discharge coefficient as a function of discharge rate for all channels modeled separately

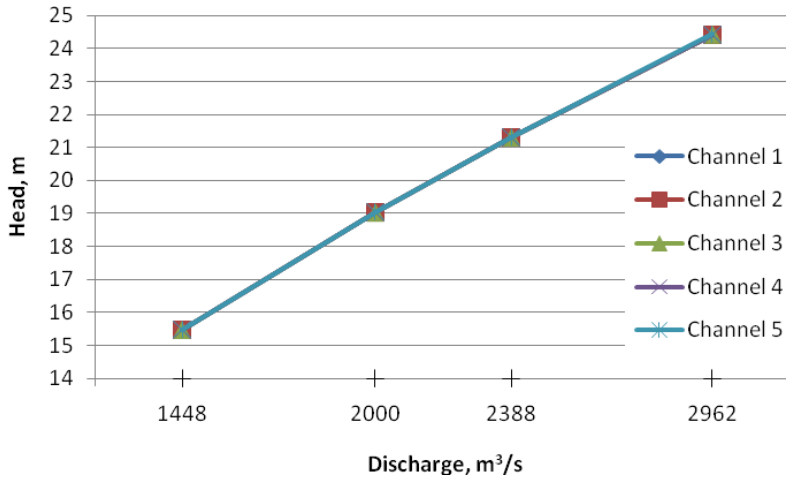

Figure 16. Head as a function of discharge rate for all channels modeled separately

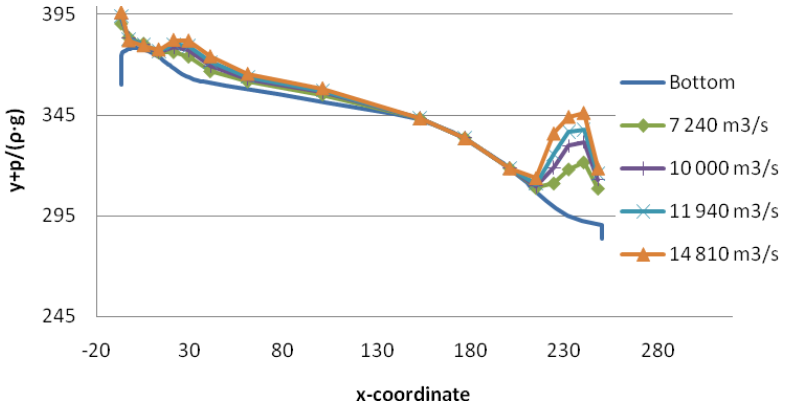

Figure 17a. The numerical pressure distribution in the separately modeled Channel 3 for the four discharge rates

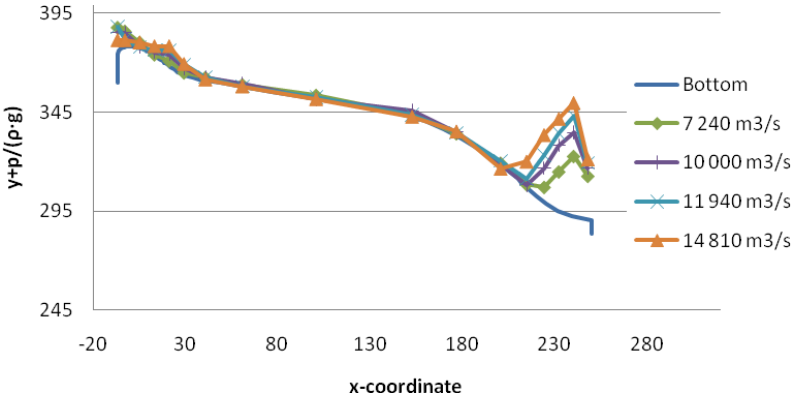

Figure 17b. The pressure distribution from the scale model for the four discharge rates

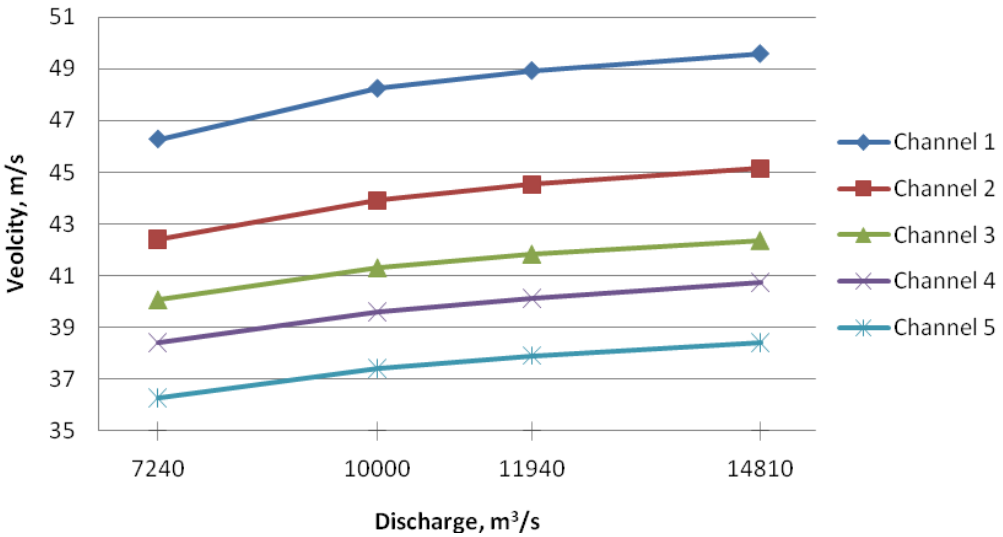

Figure 18. The maximum velocity at the outlet for all channels modeled separately as a function of discharge rate

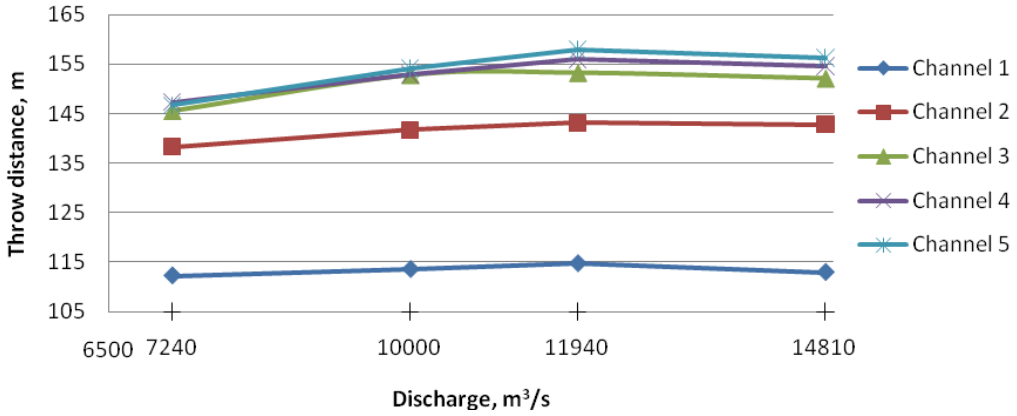

Figure 19. Jet throw distance for all channels as a function of discharge rate

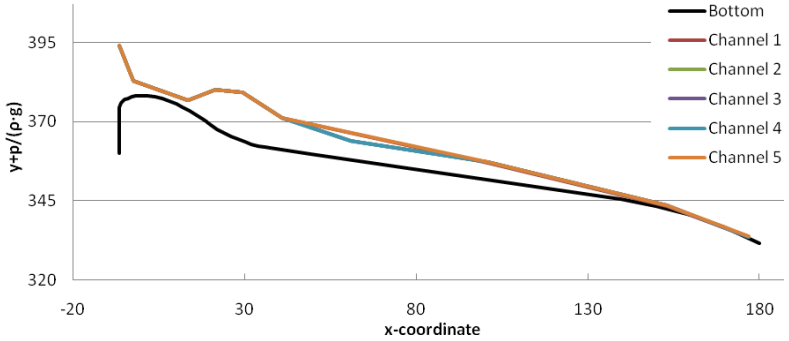

Figure 20. The numerical static pressure distribution for Channel 1-5, modeled separately, up to x=180m, 11 940 m3/s

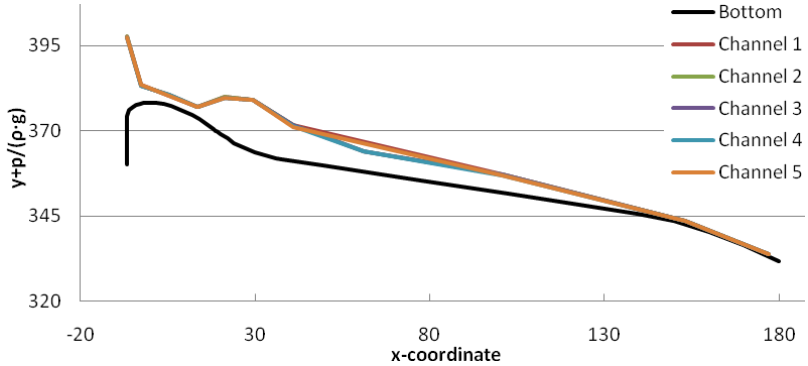

Figure 21. The numerical static pressure distribution for Channel 1-5, modeled together, up to x=180m, 11 940 m3/s

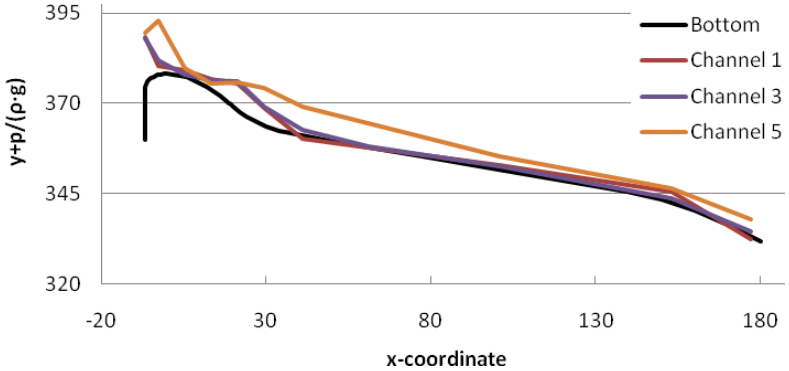

Figure 22. The static pressure distribution for Channel 1-5 from the scale model up to x=180m, 11 940 m3/s

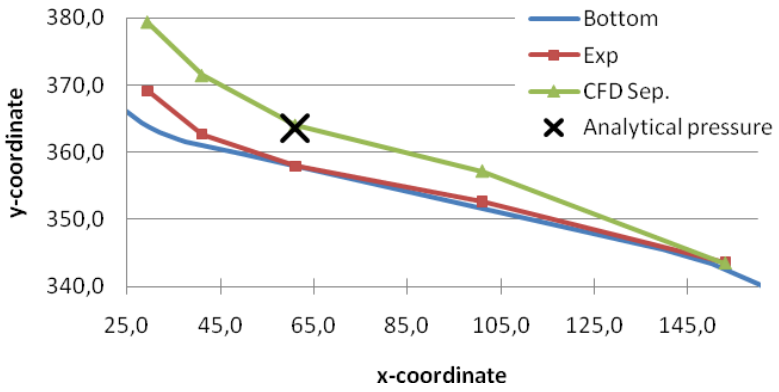

Figure 23. The numerical pressure distribution, the pressure distribution from the scale model and the analytical pressure at the inflection point in Channel 3, 11 940 m3/s

Table 15. Final results and validation pressures compared to scale model data in Channel 1. Two pressures from the scale model are negative and thus no difference in percent is presented

Point	Standard	Mod. 1	Mod. 2	Mod. 3	Mod. 4	Mod. 5	Mod. 6
1	44%	44%	44%	48%	31%	43%	45%
2	87%	88%	88%	85%	65%	86%	88%
3	37%	37%	38%	36%	19%	38%	38%
4	9%	9%	9%	8%	5%	9%	9%
5	61%	61%	61%	61%	65%	62%	61%
6	224%	224%	224%	224%	228%	225%	224%
7	-	-	-	-	-	-	-
8	306%	306%	306%	306%	303%	311%	306%
9	-69%	-69%	-69%	-70%	-71%	-67%	-69%
10	-	-	-	-	-	-	-
11	-78%	-78%	-78%	-78%	-78%	-71%	-77%
12	-40%	-40%	-39%	-39%	-38%	-39%	-39%
13	35%	35%	35%	36%	37%	36%	35%
14	23%	23%	23%	25%	32%	24%	23%
15	71%	71%	71%	71%	69%	72%	71%
16	0%	0%	0%	0%	0%	-1%	-1%
17	-30%	-30%	-30%	-30%	-34%	-32%	-31%

5. DISCUSSION

Limited computational power constrained the number of cells that was possible to use in the simulations. With no limitations, a better model could be built with the five channels together with a smaller size of cells in order to find possible cross waves and perhaps a better agreement with the pressure distributions from the scale models.

In order to make a fully satisfied comparison between the numerical and the scale model results, more parameters than were used in this study should be compared. Since there are no velocity and water depths data available from the scale model it is hard to determine the validity of the results from the numerical model when all verification relies on only one hydraulic parameter. Due to this, the numerical results have to be

considered uncertain and since the comparison does not lead to a verification of the model, the emphasis of the discussion will be on the validation of the model and potential error sources.

Because of the uncertainties in the results, a couple of modifications of the settings in FLUENT were made. Most of the modifications gave similar results but modification 4, representing a second order discretization, gave results that differed from the others. But since the difference in some of the points became lower, in others remained the same or even got higher and the simulation time increased, no further time were spent using second order discretization.

5.1. Fault tree analysis of disagreement between models

There are a number of factors which might affect the agreement between the numerical modeling and the scale model. To aid the analysis of the disagreement, a fault tree was constructed and can be found in Appendix D. The discussion below is based upon the created fault tree.

There are three possible reasons to why the pressure distributions differ: the pressure distribution in the numerical model is incorrect, the pressure distribution in the scale model is incorrect and both pressure distributions are incorrect.

5.1.1. *Pressure distribution in numerical model is incorrect*

The first branch of the fault tree is the most probable cause of disagreement and treats the case when the numerical model is incorrect but the scale model is correct. There are two possible reasons to why the numerical model is incorrect, errors in the pre-processing stage and in the solving stage.

Errors in the pre-processing stage

Errors in the pre-processing stage can be due to misplaced boundaries or misuse of symmetry, errors in channel geometry or errors in the discretization.

The boundaries are probably correctly placed in this study, far enough from the crests to obtain an unaffected upstream water level and along natural margins for the other boundaries. The use of symmetry might on the other hand have been a mistake. The symmetry plane along the longitudal center of the channels effectively prevents any possible cross waves or snaking wave pattern to form. There might be differences in channel geometry between the numerical model and the scale model due to contradicting and incomplete documentation from the scale model. However, the effect on the pressure distribution is probably small. The final possible error source from the pre-processing stage is the discretization. The mesh is, due to computational power, far too coarse. This is by far the most probable cause of the bad agreement with the pressure distribution from the scale model.

Errors in the solving stage

Errors in the solving stage can be due to unsuitable choice of solver, models and settings.

The choice of solver can be crucial but FLUENT is approved commercial software and has good references from older projects, for example Margeirsson (2007), Halldén (2010) and Li et al (2007), so the choice of solver should not affect the results. To be able to treat the free surface the VOF-method was used and the k-e model was chosen as turbulence model. Both models have been thoroughly verified and approved in other reports (Dargahi, 2006) and can be considered to be

accurate enough for this project. To validate the settings in FLUENT, a series of sensitivity tests were carried out and are presented in the results section. The tests show that the numerical model is practically unaffected by changes in settings which indicates that something is wrong with the model.

5.1.2. *Pressure distribution in scale model is incorrect*

The second branch of the fault tree is not as probable as the first but will be discussed anyway. The second branch treats the case when the numerical model is correct and the scale model is incorrect. There are two possible reasons to why the scale model is incorrect, errors in the setup of the model and in the measurement of the pressures.

Errors in the setup

Errors in the scale model setup can be due to misplaced boundaries and incorrect channel geometry.

There is no evidence that the boundaries have been placed poorly in the scale model test and even though the documentation of the model geometry is limited there is no reason to believe that there are any errors in the results due to this cause.

Errors in measurements

Errors in measurements can be due to problems of separating the static pressure from the dynamic and to find representative spots for pressure measuring.

If, accidentally, a part of the velocity head is included in the measurement of the static pressure, the result will be too high. In this study, the pressure distribution from the scale model is much lower than the pressure distribution from the numerical model which indicates that the problem is something else. The report from the scale model indicated the occurrence of cross waves in the channels which might affect the pressure.

Errors in model

Scale effects are a phenomenon where water behaves different in different scales. Water tends to act more viscous in small scales than in prototypes and sometimes a modification of the water chemistry is needed to make the water behave as in full scale structures (Yang, 2010). No information about any modification of the water chemistry has been found in the Shibuya scale model but there is on the other hand no reason to believe that scale effects alone are responsible for the deviation in pressure distributions.

5.1.3. *Pressure distribution in both models is incorrect*

The last branch treats the case when both the numerical and the scale model are incorrect. This alternative contains all error sources from the previous branches but as stated earlier, the most predominant error source is most likely the cell size and the contribution from errors in the scale model are probably negligible.

5.2. Discharge capacity

This study indicates that the discharge capacity for the five different spillway channels is practically the same for all discharge rates. This was expected because all channels have the same geometry in the area which influences the discharge capacity and the same boundary conditions were used for all channels in the numerical model.

In the model with all five channels modeled together, the discharge coefficient for the spillway system is slightly smaller than with each channel modeled separately. Less emphasis should be put upon the results from the model with all channels because of the extremely coarse mesh. Still, when comparing the coefficients from the model with five channels modeled together with the discharge data from the scale model, which unfortunately only could be made for the two largest discharge rates, they showed a good agreement.

There is however a big difference in discharge capacity and surface elevation between the separately modeled channels and the scale model. This means that the separately modeled numerical models discharge water easier than the scale model. The scale model results might contain a small amount of error due to scale effects, for example water tends to act more viscous in small scales than in large scales (Yang, 2010). It should be mentioned that the discharge capacities from the scale model are based on discharge rates and unaffected upstream water levels and there is no information about the accuracy of these data.

One of the major error sources, besides errors in the numerical model which are discussed in 5.1.1 Pressure distribution in numerical model is incorrect, is how the water surface is defined in the post-processing stage. This error mostly depends on the mesh density, since coarse mesh leads to a very diffuse water surface. If the water surface is diffuse, like in this study, the volume fraction of water which represents the water surface must be defined. With an infinitesimal mesh size the error of the water surface elevation would also be infinitesimal but, on the other hand, that would also mean an unmanageable amount of cells.

The technique of how to determine the water surface used in this study is not confirmed in other projects and might not always be applicable. But in this study, with such high heads, an error of the surface elevation with a few centimeters would only change the discharge coefficient marginally.

5.3. **Pressure distribution**

As can be seen in the results the agreement between the numerical and the scale model pressure distributions differ along the channels. In the first and last parts of the channels the agreement is acceptable but in the middle there are large percental differences. By observing all of the results in Appendix B, one can see that the pressure distribution trends in the numerical analysis and the scale model resembles each other but the scale model pressures in points 5-8 and are much lower than the numerical results.

The results from the theoretical investigation show a similar pressure as the numerical modeling produce. This, along with an observed vector plot in FLUENT, confirm that the numerical simulation generates a simple flow pattern with parallel streamlines in contradiction to the scale model in which cross waves and snaking streamlines were observed. This unstable flow pattern was not detected in FLUENT probably due to the coarse mesh and the use of symmetry planes.

Even though the agreement between the numerical results and the scale model data is quite low in about half of the points along the channel, it was noted that the numerical simulations gave very similar pressure distributions the first part in each separately modeled channel at the same discharge rate. This phenomenon also occurred in the model where all five channels were modeled together, but could not be observed in the scale model data which from the parametric study show a strongly

fluctuating pressure distribution. Just as in the discussion about the discharge capacity, the similar pressure distribution from the numerical models in the beginning of each channel is probably due to the identical geometry and boundary conditions. It is a bit strange though that the pressure distribution is similar for all five channels when they are modeled together, but that is probably due to the inability of the software to simulate the complex hydraulic situation in the channels with such a coarse mesh.

5.4. Flip bucket throw distance

Since there are no scale model data available for comparing the throw distances, the only validation of the calculated throw lengths could be made by using more than one equation. It was shown that results from equation (5) were approximately in the middle of the span that was calculated from equation (4). From this point of view the results may be considered as verified as equation (5) gives the length to the middle of the jet plunging into the downstream water. But, it is very important to point at the errors that exists in the equations and the including parameters.

There are discussions about how to determine jet flow trajectories in hydraulic journals and many different equations has been presented and criticized. Hence, the results from the equations used in this study should not be taken as absolutely true but might together give a good approximation of the throw distance.

One important error source when discussing errors in the equation parameters is that the free water surface level is quite diffuse at the outlet, especially when such a coarse mesh was used as in this study. Hence, the water velocity at the surface is very hard to define at the outlet. The initial angle of the jet flow was measured by hand from a velocity vector field and errors may occur according to this primitive procedure. But since finding the throw distances was not the main task of this study, the authors think a simplification like this can be accepted. Noticeable is that a not presented sensitivity test showed that a small difference in initial angle hardly changed the throw distance at all.

It can be concluded from the parametric study that the velocity at the outlet is proportional to the discharge rate and the vertical distance from the crest, therefore the maximum velocity at the outlets is highest for Channel 1 and lowest for Channel 5. Interesting is that the empirical equations gave similar throw lengths for all discharge rates. This is due to the great influence of the downstream water elevation in the used equations.

The shortest span is produced by Channel 5 and the channel also has its outlet positioned at the highest elevation of the outlets and thus, plunging pool erosion should be most serious at the location of the plunging jet from Channel 5. Noticeable is also that the longest throw distance came from Channel 5, even though it had the lowest velocity at the outlet compared to the other channels.

6. CONCLUSION

CFD-modeling is more and more used in hydraulic design and the user-friendly software of today gives practically everyone with basic knowledge in computers and hydraulics ability to make up their own CFD model. If a numerical model is created by a person without necessary knowledge in hydraulics and numerical modeling and the results are used without verification, fatal mistakes can be made.

Therefore, as long as the users of CFD software lack essential knowledge in the principal areas, the results must be validated by scale models or prototype data. The verification data should consist of at least two different hydraulic parameters to guarantee a correct verification of the numerical model.

The computational power along with the delimitation potential determines the maximum size of the prototype. If the prototype is too big and the hydraulic and geometrical conditions do not permit the necessary delimitation, the numerical model might not be possible to generate accurate results because of the size of the cells.

The discharge investigation showed that the five different channels have similar discharge capacity. There is however a quite large deviation from the scale model results for the highest discharge rate. The deviation may to the main part depend on uncertainties in the discharge capacity from the scale model. Another part of the deviation may be scale effects causing the water to be more viscous in the scale model.

The pressure distributions achieved in this study are realistic but comparison with results from the scale model, which is such a robust and traditionally accepted method, shows significant deviations. Thus one must be critical to the results. Further work with verification of numerical models of hydraulic structures with extreme and complex geometries should be performed.

The calculations of the jet flow throw distances from the flip buckets resulted in different spans and the smallest span was caused by Channel 5, which also had the longest throw distance. Unfortunately, there are no scale model data to compare the results with and no studies using the same empirical equations with hydraulic conditions similar to this study were found. Therefore the results cannot be used without further investigations.

7. REFERENCES

Chung T. J. (2002) Computational fluid dynamics. The press syndicate of the University of Cambridge. 1036 p

Dargahi B. (2006) Experimental Study and 3D Numerical Simulation for a Free-Overflow Spillway. *Journal of Hydraulic Engineering*. Vol 132 No 9 pp 899-907

Drazin P. & Riley N. (2006) The Navier-Stokes Equations – A Classification of Flows and Exact Solutions. Cambridge University Press. 196 p

Fefferman C. (2006) Existence and smoothness of the Navier-Stokes equation. *The Milennium prize problems*. Clay Mathematics Institute. pp 56-68

FLUENT Inc. (2006) FLUENT 6.3 User's guide. FLUENT Inc. 2501 p

Hanson G. & Temple D. (2007) The National Dam Safety Program - Final Report on Coordination and Cooperation with the European Union on Embankment Failure Analysis. Federal Emergency Management Agency. 168 p

Hirsch C. (2007) Numerical computation of internal & external flows. Butterworth-Heinemann. 656 p

Hirt C.W. & Nichols B.D. (1981) Volume of Fluid (VOF) Method for the Dynamics of Free Boundaries. *Journal of Computational Physics* Vol 39 pp 201-225

Häggström S. (2009) Hydraulik -för samhällsbyggnad. Liber AB. 287 p

Kim D.G. & Park J.H. (2005) Analysis of Flow Structure over Ogee-Spillway in Consideration of Scale and Roughness Effects by Using CFD Model. *KSCE Journal of Civil Engineering*. Vol 9 No 2 pp 161-169

Li L.; Chen Y. & Li Y. (2007) Three- dimensional VOF model and its application to the water flow calculation in the spillway. Journal of Hydroelectric Engineering. Vol 26 No 2 pp 83-87

Margeirsson B. (2007) Computational modeling of flow over a spillway – in Vatnsfellsstífla dam in Iceland. Department of applied mechanics, Chalmers University of technology. 30 p

Panton R. L. (2005) Incompressible flow. John Wiley & sons, Inc. 821 p

Poroseva S. & Laccarino G. (2001) Simulating separated flows using the k-ε model. Center for turbulence research. 383 p

Wahl T.L.; Frizell K.H. & Cohen E.A. (2008) Computing the Trajectory of Free Jets. *Journal of Hydraulic Engineering*. Vol 134 No 2 pp 256-260

Yang J. (2006) Modeller ger svar – på hur kraftverksdammar bör förstärkas. SwedCOLD. Nyhetsbrev No 1 p 3

Zhang Y.; Ma J. & Zheng S. (2008) An experimental study on high head and large discharge spillways with slotted flip bucket terminal structures. Hydropower. Vol 34 No 11 pp 48-51

8. OTHER REFERENCES

Li W. (2007) Handbook of hydraulic computation, China water resource and hydropower press 575 p, Book in Chinese

Sassaman T. C.; Gemperline E. J.; Halstead K. C.; Lamkin K. H. & Kocahan H. (2009) Modeling: Physical Models: Why Hydro Developers Use Them in the Computer Age. Hydroworld.com, <http://www.hydroworld.com/hrhrw/en-us/index/display/article-display.articles.hydro-review.volume-28.issue-8.articles.modeling_-physical.html> seen 2010-08-29

Yang J. Professor at the Department of Land and Water Resources Engineering at the Royal Institute of Technology, Sweden and head of Vattenfall Research & Development in Älvkarleby, Sweden. Personal communication June 2010 to September 2010

Zhang Y.L. Professor at the Department of Hydraulic Engineering, Tsinghua University, Beijing, China. Personal communication June 2010 to September 2010

APPENDIX A – GEOMETRY AND MESH

13 pages

Channel 1

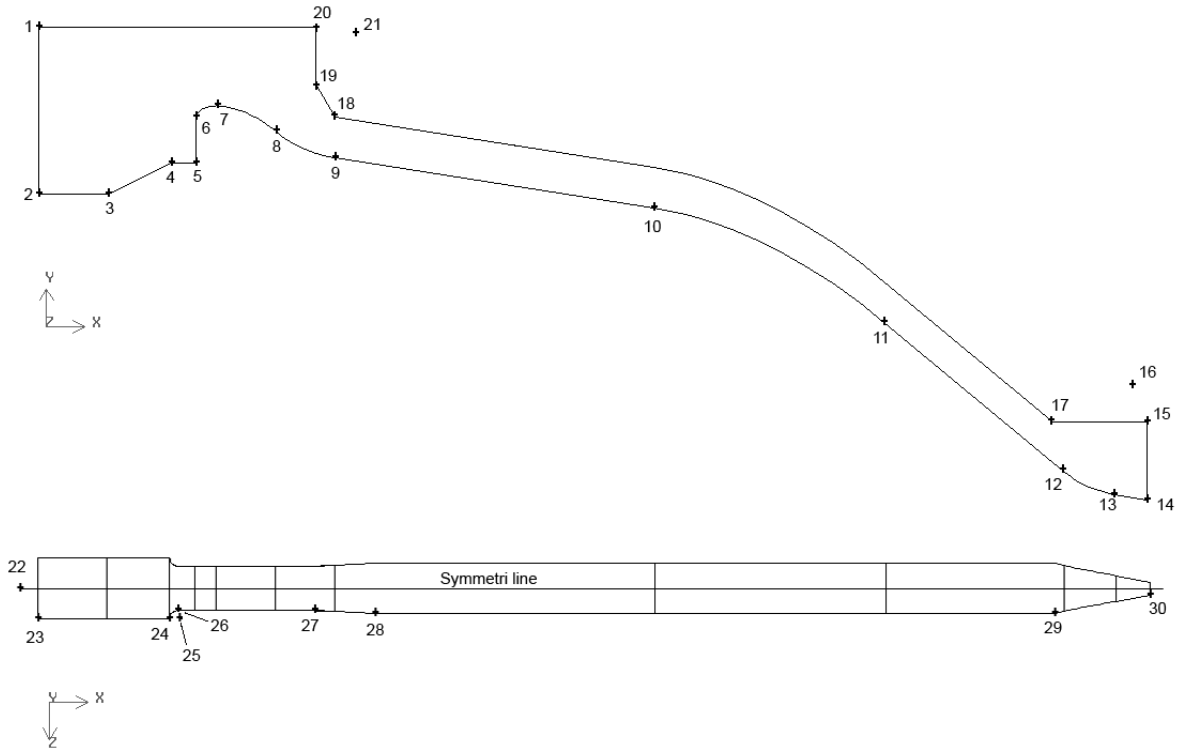

Point	x-coordinate	y-coordinate	z-coordinate	Comments
1	-56,580	403,200		
2	-56,580	350,000		
3	-34,600	350,000		
4	-14,600	360,000		
5	-6,600	360,000		
6	-6,600	374,460		
7	0,000	378,200		
8	18,771	370,000		
9	37,660	361,600		
10	139,630	345,540		
11	212,425	309,164		
12	269,000	262,020		
13	285,330	254,440		
14	296,000	252,560		
15	296,000	277,500		
16	291,410	288,910		Centerpoint line 12-13
17	266,000	277,500		
18	37,660	374,600		
19	31,400	385,000		
20	31,400	403,200		
21	43,910	401,110		Centerpoint line 8-9
22			8,000	Symmetry line
23	-56,580		17,500	
24	-14,600		17,500	
25	-12,100		17,500	Centerpoint line 24-26
26	-12,100		15,000	
27	31,400		15,000	
28	50,480		16,000	

29	266,000		16,000	
30	296,000		10,000	

Line	Expression for curvature
6-7	$\frac{x^2}{6{,}6^2}+\frac{(3{,}74-y)^2}{3{,}74^2}=1$
7-8	$y=0{,}03613\cdot x^{1{,}85}$
8-9	R= 40, centerpoint 21
10-11	$\bar{y}=0{,}1584\cdot\bar{x}+0{,}0046\cdot\bar{x}^2$ (local coordinates)
12-13	R=35, centerpoint 16
All other nodes are connected with straight lines	

Points where the static pressure were determined			
Point	**x-coordinate**	**y-coordinate**	**z-coordinate**
1	-6,6	374,46	8
2	-2,6	377,89	8
3	5,4	377,372	8
4	13,4	373,797	8
5	21,4	368,054	8
6	29,4	363,843	8
7	41	361,071	8
8	101	351,569	8
9	153	342,432	8
10	177	332,909	8
11	201	318,07	8
12	229	295,353	8
13	257	272,02	8
14	270	261,223	8
15	278	256,579	8
16	286	254,322	8
17	294	252,913	8

Channel 2

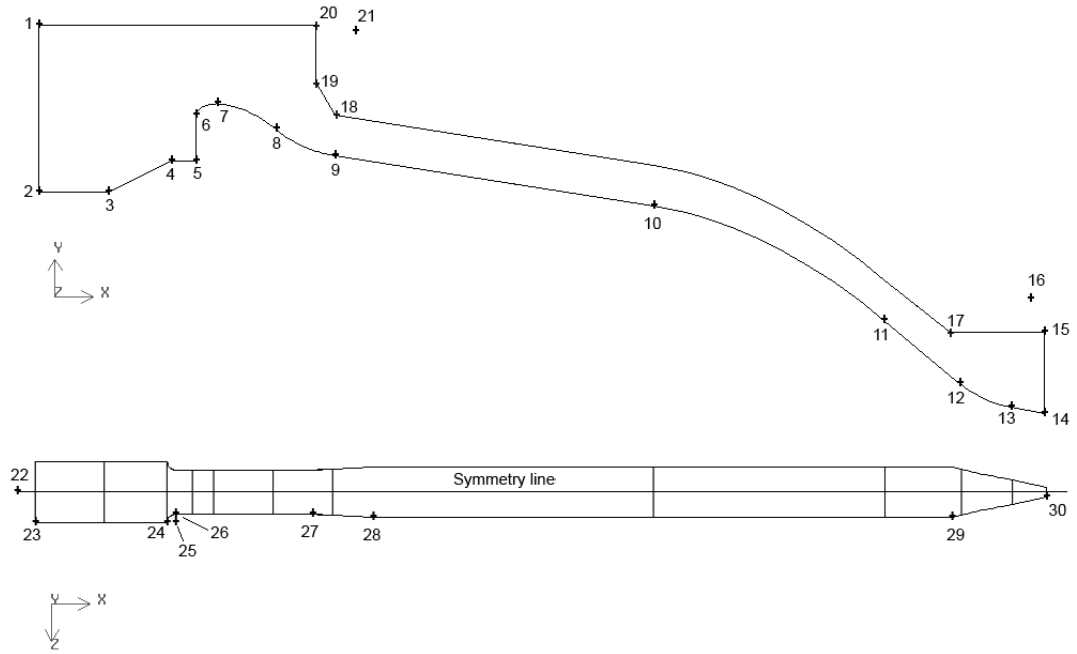

Point	x-coordinate	y-coordinate	z-coordinate	Comments
1	-56,580	403,200		
2	-56,580	350,000		
3	-34,600	350,000		
4	-14,600	360,000		
5	-6,600	360,000		
6	-6,600	374,460		
7	0,000	378,200		
8	18,771	370,000		
9	37,660	361,600		
10	139,630	345,540		
11	212,425	309,164		
12	236,501	289,101		
13	252,829	281,521		
14	263,500	279,639		
15	263,500	305,300		
16	258,907	315,989		Centerpoint line 12-13
17	233,500	305,300		
18	37,660	374,600		
19	31,400	385,000		
20	31,400	403,200		
21	43,910	401,110		Centerpoint line 8-9
22			27,000	Symmetry line
23	-56,580		36,500	
24	-14,600		36,500	
25	-12,100		36,500	Centerpoint line 24-26
26	-12,100		34,000	
27	31,400		34,000	
28	50,480		35,000	
29	233,500		35,000	
30	263,500		28,600	

Line	Expression for curvature
6-7	$\frac{x^2}{6{,}6^2} + \frac{(3{,}74 - y)^2}{3{,}74^2} = 1$
7-8	$y = 0{,}03613 \cdot x^{1{,}85}$
8-9	R= 40, centerpoint 21
10-11	$\bar{y} = 0{,}1584 \cdot \bar{x} + 0{,}0046 \cdot \bar{x}^2$ (local coordinates)
12-13	R=35, centerpoint 16
All other nodes are connected with straight lines	

Points where the static pressure were determined			
Point	**x-coordinate**	**y-coordinate**	**z-coordinate**
1	-6,6	374,46	27
2	-2,6	377,89	27
3	5,4	377,379	27
4	13,4	373,803	27
5	21,4	368,054	27
6	29,4	363,843	27
7	41	361,071	27
8	61	357,904	27
9	101	351,569	27
10	153	342,437	27
11	177	332,91	27
12	201	318,083	27
13	227,5	296,603	27
14	237,5	288,305	27
15	245,5	283,663	27
16	253,5	281,403	27
17	261,5	279,992	27

Channel 3

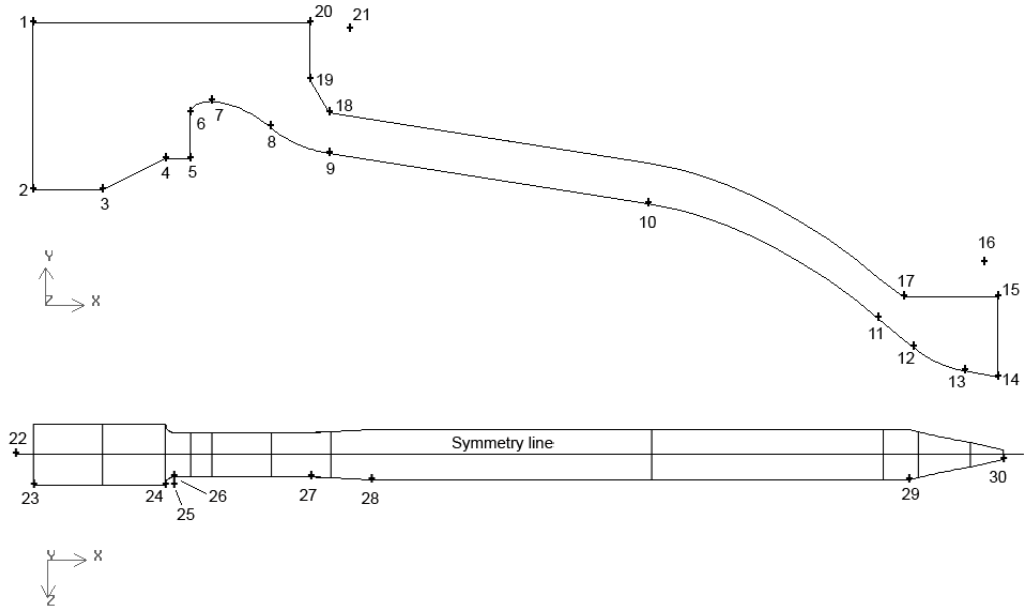

Point	x-coordinate	y-coordinate	z-coordinate	Comments
1	-56,580	403,200		
2	-56,580	350,000		
3	-34,600	350,000		
4	-14,600	360,000		
5	-6,600	360,000		
6	-6,600	374,460		
7	0,000	378,200		
8	18,771	370,000		
9	37,660	361,600		
10	139,630	345,540		
11	212,425	309,164		
12	223,501	299,935		
13	239,829	292,355		
14	250,500	290,473		
15	250,500	315,920		
16	245,906	326,823		Centerpoint line 12-13
17	220,500	315,920		
18	37,660	374,600		
19	31,400	385,000		
20	31,400	403,200		
21	43,910	401,110		Centerpoint line 8-9
22			46,000	Symmetry line
23	-56,580		55,500	
24	-14,600		55,500	
25	-12,100		55,500	Centerpoint line 24-26
26	-12,100		53,000	
27	31,400		53,000	
28	50,480		54,000	
29	220,500		54,000	
30	250,500		47,600	

Line	Expression for curvature
6-7	$\frac{x^2}{6{,}6^2} + \frac{(3{,}74 - y)^2}{3{,}74^2} = 1$
7-8	$y = 0{,}03613 \cdot x^{1{,}85}$
8-9	R= 40, centerpoint 21
10-11	$\bar{y} = 0{,}1584 \cdot \bar{x} + 0{,}0046 \cdot \bar{x}^2$ (local coordinates)
12-13	R=35, centerpoint 16
All other nodes are connected with straight lines	

Points where the static pressure were determined			
Point	**x-coordinate**	**y-coordinate**	**z-coordinate**
1	-6,6	374,46	46
2	-2,6	377,89	46
3	5,4	377,379	46
4	13,4	373,803	46
5	21,4	368,05	46
6	29,4	363,837	46
7	41	361,071	46
8	61	357,904	46
9	101	351,569	46
10	153	342,432	46
11	177	332,91	46
12	201	318,071	46
13	215	307,019	46
14	224,5	299,137	46
15	232,5	294,493	46
16	240,5	292,237	46
17	248,2	290,879	46

Channel 4

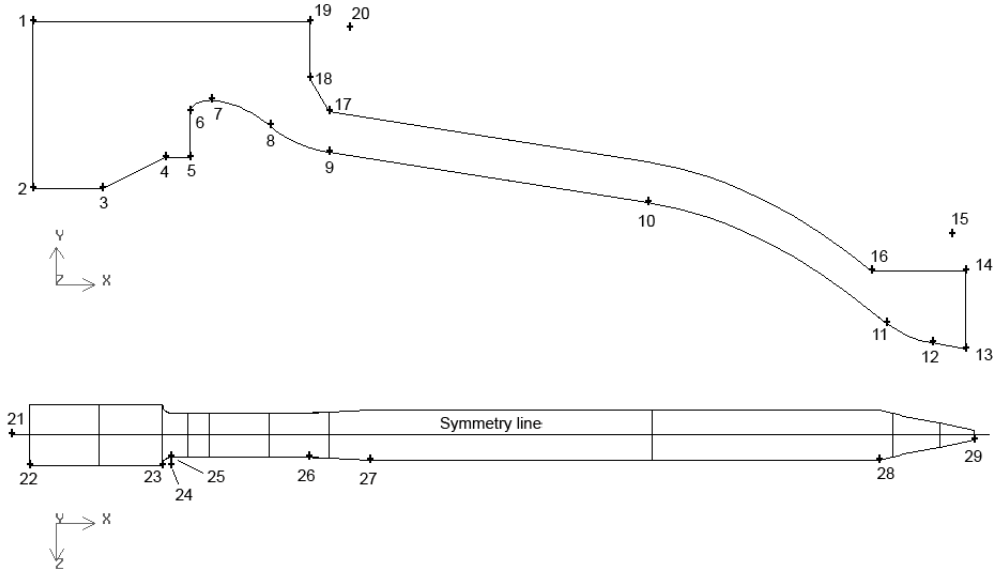

Point	x-coordinate	y-coordinate	z-coordinate	Comments
1	-56,580	403,200		
2	-56,580	350,000		
3	-34,600	350,000		
4	-14,600	360,000		
5	-6,600	360,000		
6	-6,600	374,460		
7	0,000	378,200		
8	18,771	370,000		
9	37,660	361,600		
10	139,630	345,540		
11	214,915	307,177		
12	229,629	300,864		
13	240,300	298,980		
14	240,300	323,920		
15	235,707	335,322		Centerpoint line 11-12
16	210,300	323,920		
17	37,660	374,600		
18	31,400	385,000		
19	31,400	403,200		
20	43,910	401,110		Centerpoint line 8-9
21			65,000	Symmetry line
22	-56,580		74,500	
23	-14,600		74,500	
24	-12,100		74,500	Centerpoint line 23-25
25	-12,100		72,000	
26	31,400		72,000	
27	50,480		73,000	
28	210,300		73,000	
29	240,300		66,600	

Line	Expression for curvature
6-7	$\frac{x^2}{6{,}6^2} + \frac{(3{,}74 - y)^2}{3{,}74^2} = 1$
7-8	$y = 0{,}03613 \cdot x^{1{,}85}$
8-9	R= 40, centerpoint 20
10-11	$\bar{y} = 0{,}1584 \cdot \bar{x} + 0{,}0046 \cdot \bar{x}^2$ (local coordinates)
11-12	R=35, centerpoint 15
All other nodes are connected with straight lines	

Points where the static pressure were determined			
Point	**x-coordinate**	**y-coordinate**	**z-coordinate**
1	-6,6	374,46	65
2	-2,6	377,89	65
3	5,4	377,379	65
4	13,4	373,803	65
5	21,4	368,054	65
6	29,4	363,843	65
7	41	361,071	65
8	61	357,904	65
9	101	351,569	65
10	153	342,437	65
11	177	332,913	65
12	201	318,075	65
13	208,3	312,508	65
14	214,3	307,679	65
15	222,3	303,008	65
16	230,3	300,746	65
17	238,3	299,334	65

Channel 5

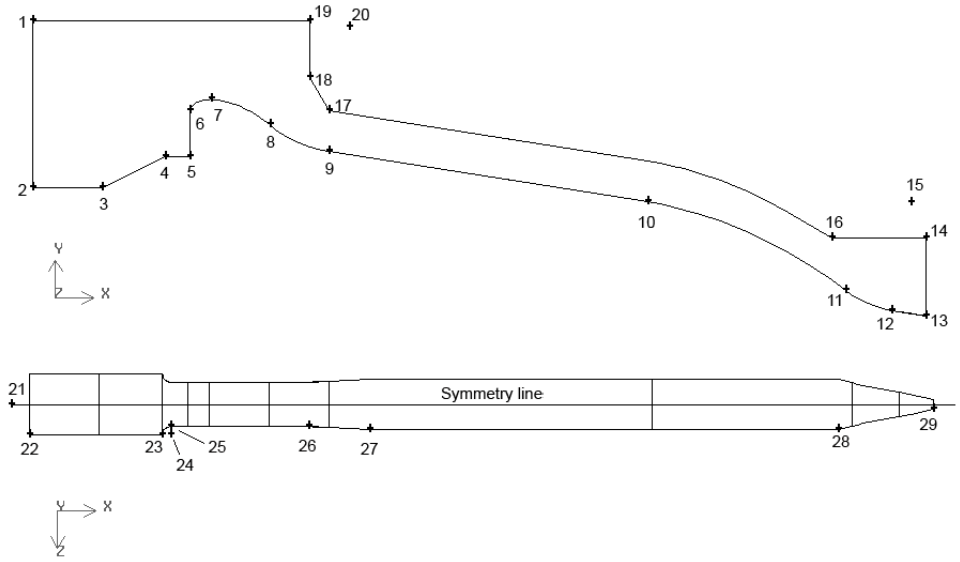

Point	x-coordinate	y-coordinate	z-coordinate	Comments
1	-56,580	403,200		
2	-56,580	350,000		
3	-34,600	350,000		
4	-14,600	360,000		
5	-6,600	360,000		
6	-6,600	374,460		
7	0,000	378,200		
8	18,771	370,000		
9	37,660	361,600		
10	139,630	345,540		
11	202,115	317,277		
12	216,829	310,964		
13	227,500	309,080		
14	227,500	334,020		
15	222,907	345,422		Centerpoint line 11-12
16	199,500	334,020		
17	37,660	374,600		
18	31,400	385,000		
19	31,400	403,200		
20	43,910	401,110		Centerpoint line 8-9
21			84,000	Symmetry line
22	-56,580		93,500	
23	-14,600		93,500	
24	-12,100		93,500	Centerpoint line 23-25
25	-12,100		91,000	
26	31,400		91,000	
27	50,480		92,000	
28	197,500		92,000	
29	227,500		85,600	

Line	Expression for curvature
6-7	$\frac{x^2}{6{,}6^2}+\frac{(3{,}74-y)^2}{3{,}74^2}=1$
7-8	$y=0{,}03613\cdot x^{1{,}85}$
8-9	R= 40, centerpoint 20
10-11	$\bar{y}=0{,}1584\cdot\bar{x}+0{,}0046\cdot\bar{x}^2$ (local coordinates)
11-12	R=35, centerpoint 15
All other nodes are connected with straight lines	

Points where the static pressure were determined			
Point	**x-coordinate**	**y-coordinate**	**z-coordinate**
1	-6,6	374,46	84
2	-2,6	377,89	84
3	5,4	377,379	84
4	13,4	373,803	84
5	21,4	368,05	84
6	29,4	363,837	84
7	41	361,071	84
8	101	351,569	84
9	153	342,437	84
10	177	332,909	84
11	189	326,164	84
12	195,5	321,931	84
13	201,5	317,718	84
14	209,5	313,106	84
15	217,5	310,846	84
16	225,5	309,434	84

Mesh, one channel separately

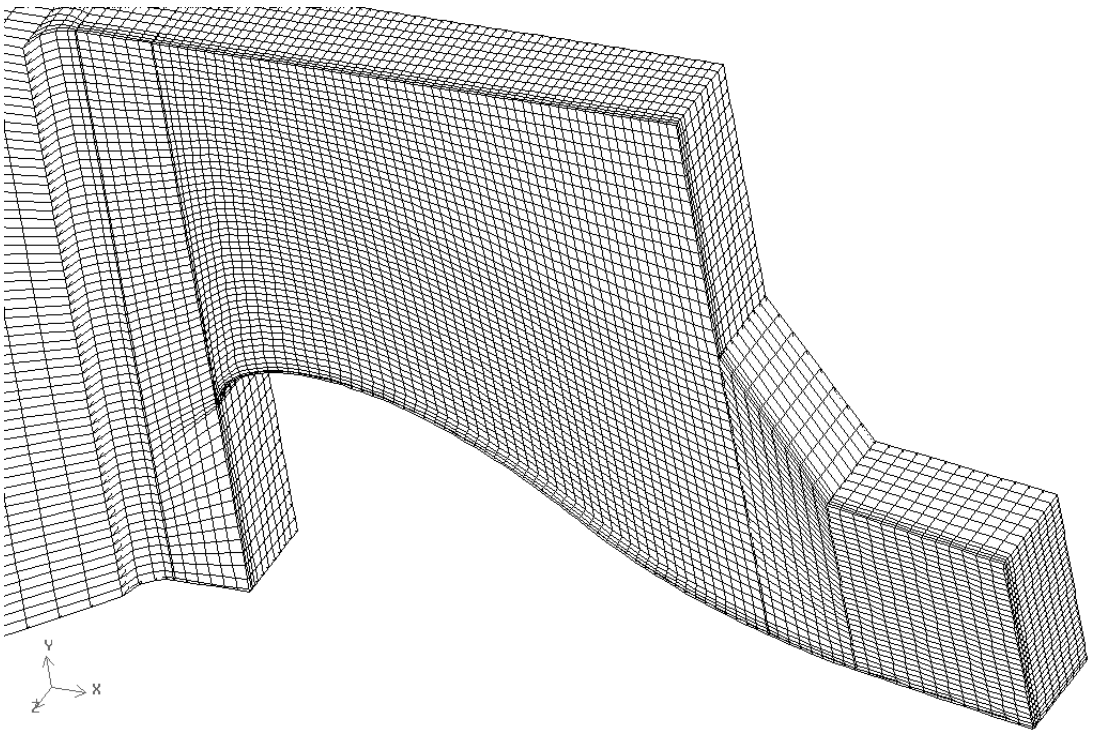

Geometry and mesh, spillway system

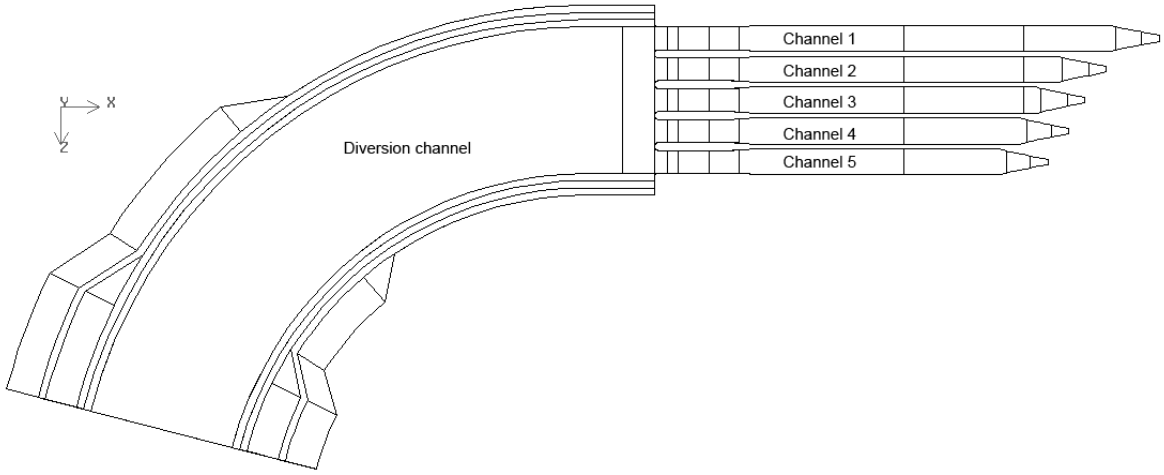

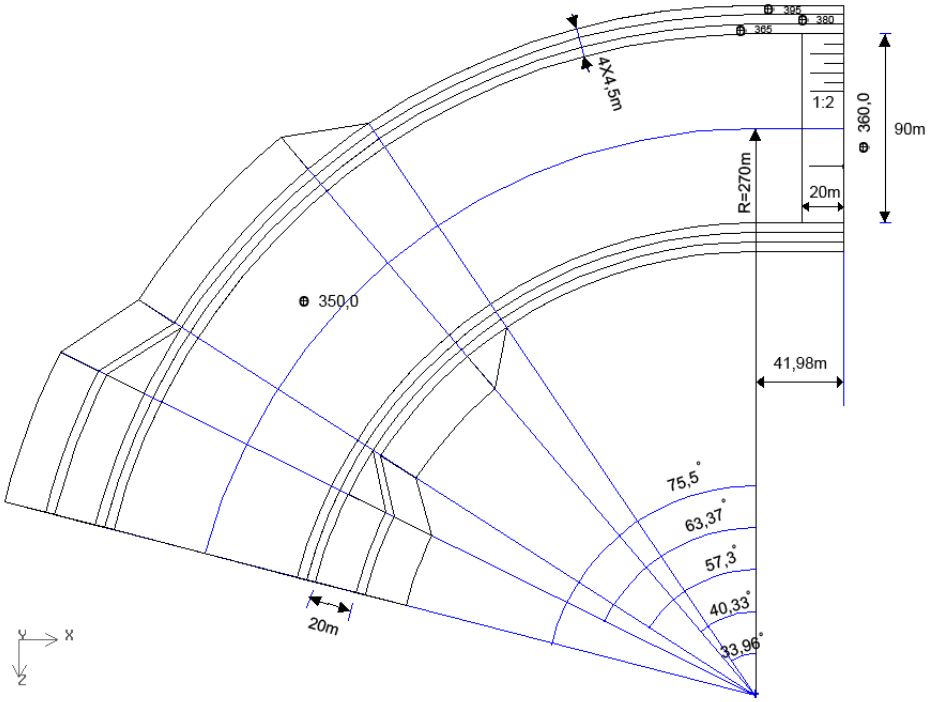

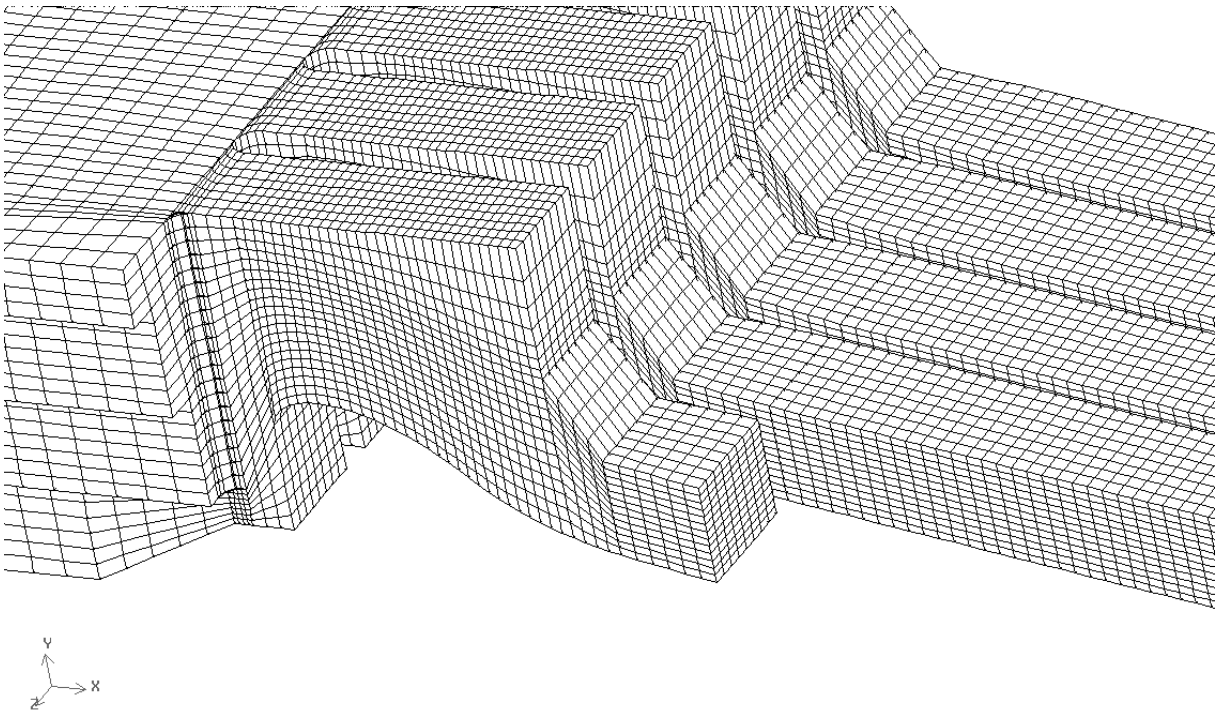
Y
X
Z

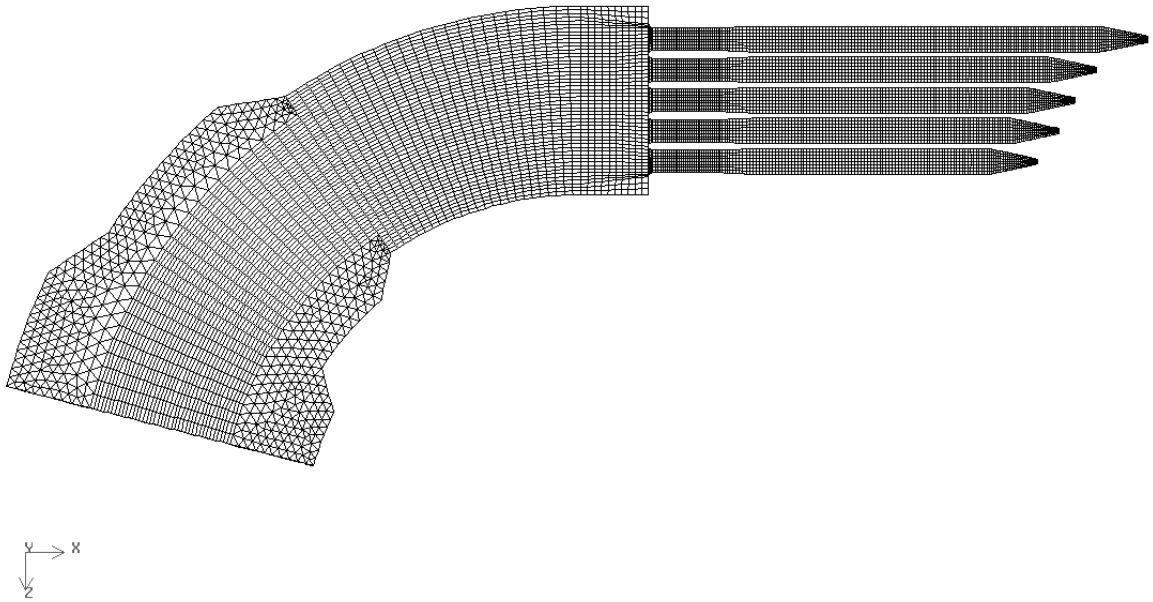
Y
X
Z

APPENDIX B – RESULTS STATIC PRESSURE

20 pages

Channel 1

7240 m^3/s					Channel 1
	Exp. Data	CFD one channel separately		CFD five channels simultaneously	
Point	p (kPa)	p (kPa)	$\Delta p/p_{exp}$	p (kPa)	$\Delta p/p_{exp}$
1	125,1	157,1	26%	179,5	43%
2	20,1	55,1	174%	58,5	192%
3	7,5	30,1	300%	32,8	336%
4	-13,3	21,8	-	21,9	-
5	35,1	80,3	129%	78,8	125%
6	18,6	99,8	438%	99,8	437%
7	6,5	54,5	732%	59,8	813%
8	20,3	35,0	73%	35,1	73%
9	45,1	7,8	-83%	9,3	-79%
10	-1,7	5,7	-	7,3	-
11	35,9	4,2	-88%	5,6	-85%
12	9,7	18,7	94%	18,3	89%
13	35,4	16,2	-54%	16,4	-54%
14	151,9	108,7	-28%	113,6	-25%
15	317,8	219,0	-31%	235,7	-26%
16	237,1	262,3	11%	260,0	10%
17	204,9	131,4	-36%	117,5	-43%

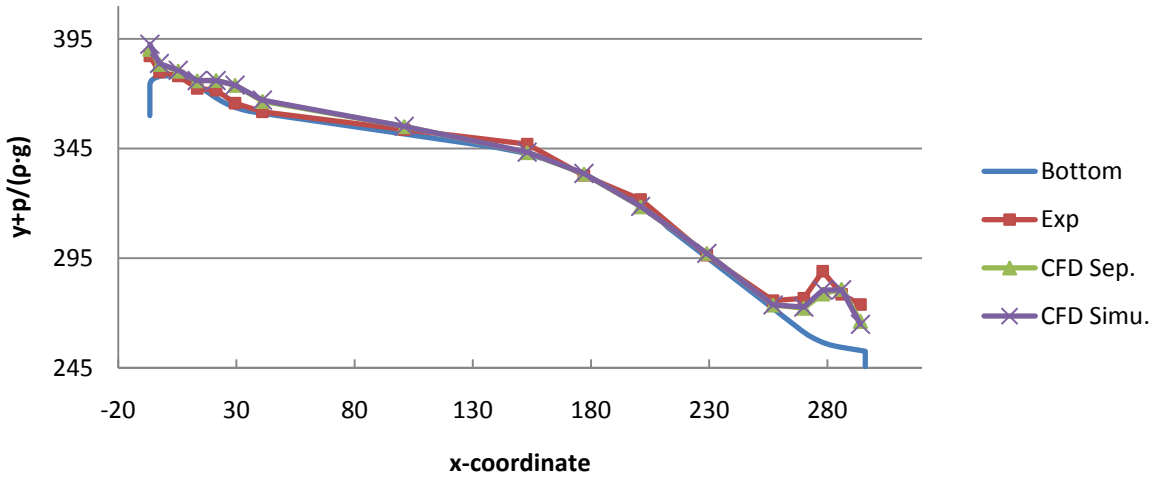

10000 m^3/s					Channel 1
	Exp. Data	CFD one channel separately		CFD five channels simultaneously	
Point	p (kPa)	p (kPa)	$\Delta p/p_{exp}$	p (kPa)	$\Delta p/p_{exp}$
1	134,9	180,2	34%	210,8	56%
2	23,0	52,3	127%	56,9	148%
3	1,6	27,3	1562%	30,9	1780%
4	15,1	26,5	76%	27,0	79%
5	59,6	104,2	75%	102,3	72%
6	31,3	132,2	322%	131,8	321%
7	3,6	80,9	2139%	86,2	2285%
8	2,7	46,6	1656%	46,6	1658%
9	53,9	8,8	-84%	10,3	-81%
10	-1,7	6,2	-	8,0	-
11	40,8	4,6	-89%	6,0	-85%
12	13,6	24,8	83%	24,4	80%
13	24,7	22,0	-11%	22,3	-10%
14	131,4	173,7	32%	174,7	33%
15	383,4	337,2	-12%	345,4	-10%
16	383,0	368,0	-4%	367,6	-4%
17	240,1	171,8	-28%	155,7	-35%

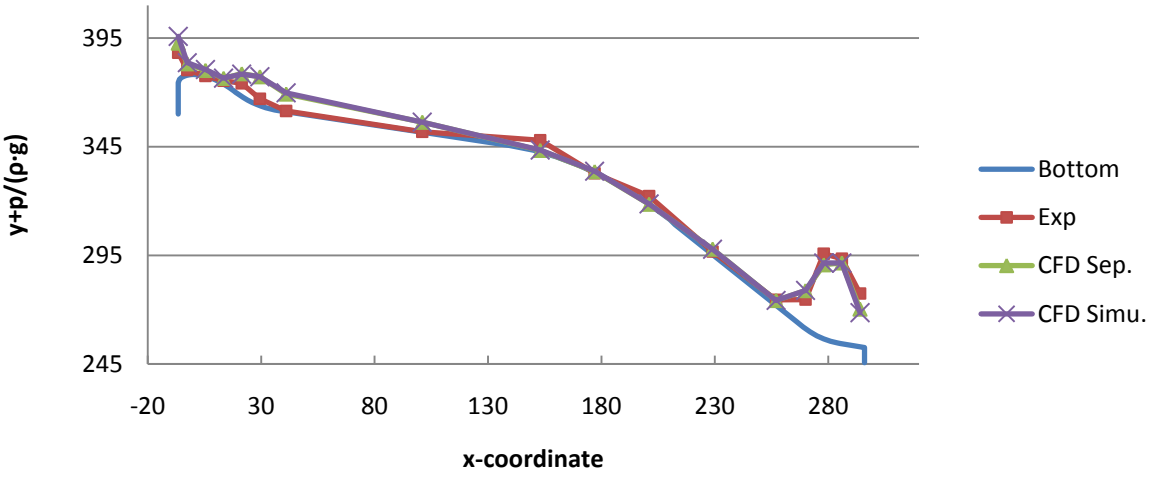

11940 m^3/s					Channel 1
	Exp. Data	CFD one channel separately		CFD five channels simultaneously	
Point	p (kPa)	p (kPa)	$\Delta p/p_{exp}$	p (kPa)	$\Delta p/p_{exp}$
1	134,9	194,2	44%	229,9	70%
2	25,9	48,6	87%	54,4	110%
3	18,3	25,1	37%	29,2	60%
4	27,8	30,3	9%	30,5	10%
5	74,3	119,4	61%	116,3	57%
6	47,0	152,2	224%	150,5	220%
7	-8,1	100,0	-	104,1	-
8	13,4	54,4	306%	54,0	302%
9	30,4	9,3	-69%	10,7	-65%
10	-3,6	6,3	-	8,1	-
11	21,2	4,7	-78%	6,2	-71%
12	47,8	28,9	-40%	28,3	-41%
13	19,8	26,7	35%	26,5	34%
14	186,2	229,8	23%	223,0	20%
15	241,4	413,8	71%	416,1	72%
16	437,8	436,3	0%	430,0	-2%
17	288,1	200,7	-30%	175,3	-39%

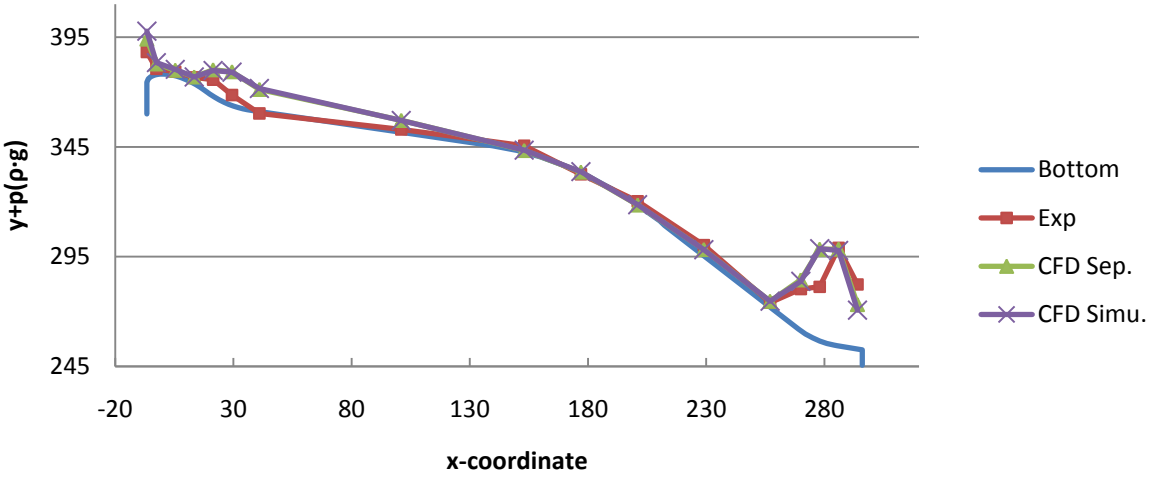

14810 m^3/s					Channel 1
	Exp. Data	CFD one channel separately		CFD five channels simultaneously	
Point	p (kPa)	p (kPa)	$\Delta p/p_{exp}$	p (kPa)	$\Delta p/p_{exp}$
1	134,9	212,4	57%	252,0	87%
2	23,0	41,0	78%	50,8	121%
3	5,6	21,8	292%	27,1	388%
4	2,4	36,7	1442%	35,1	1375%
5	57,6	139,9	143%	132,1	129%
6	64,6	178,4	176%	171,1	165%
7	-4,2	128,2	-	125,7	-
8	26,2	65,9	152%	62,7	140%
9	15,7	9,7	-38%	10,9	-31%
10	-1,7	6,0	-	8,0	-
11	21,2	4,6	-78%	6,2	-71%
12	43,0	34,9	-19%	32,8	-24%
13	23,7	35,4	49%	32,7	38%
14	151,9	322,6	112%	289,4	90%
15	383,4	512,4	34%	496,3	29%
16	400,6	535,0	34%	496,5	24%
17	248,0	237,6	-4%	195,6	-21%

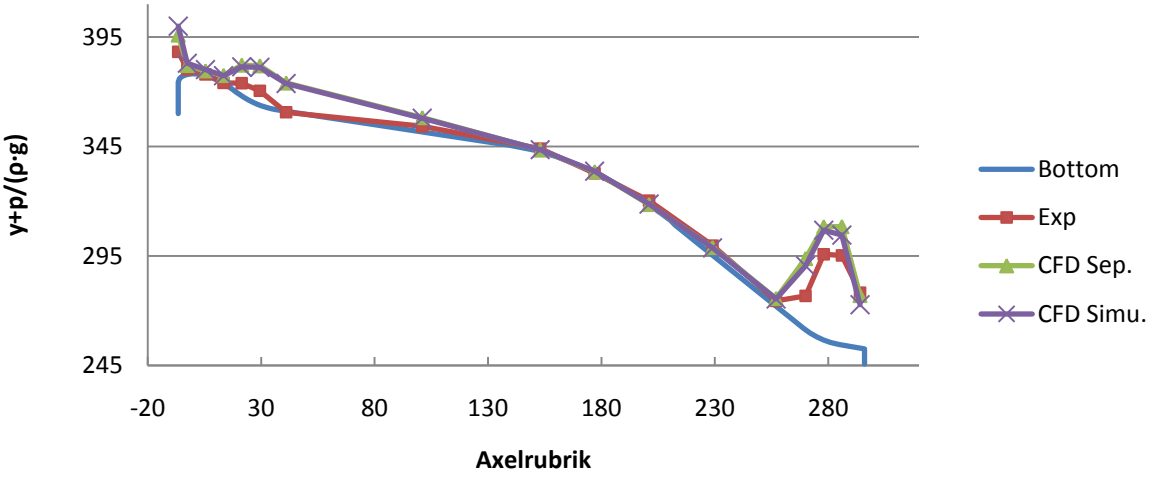

Channel 2

7240 m^3/s		Channel 2
	CFD one channel separately	CFD five channels simultaneously
Point	p (kPa)	p (kPa)
1	157,1	178,8
2	55,1	58,4
3	30,1	33,2
4	21,9	22,0
5	80,6	78,7
6	100,0	99,6
7	55,7	59,6
8	36,8	37,5
9	35,5	35,0
10	8,6	9,3
11	6,7	7,3
12	5,5	5,5
13	19,3	18,9
14	111,8	114,5
15	208,4	245,8
16	241,1	303,6
17	124,8	157,6

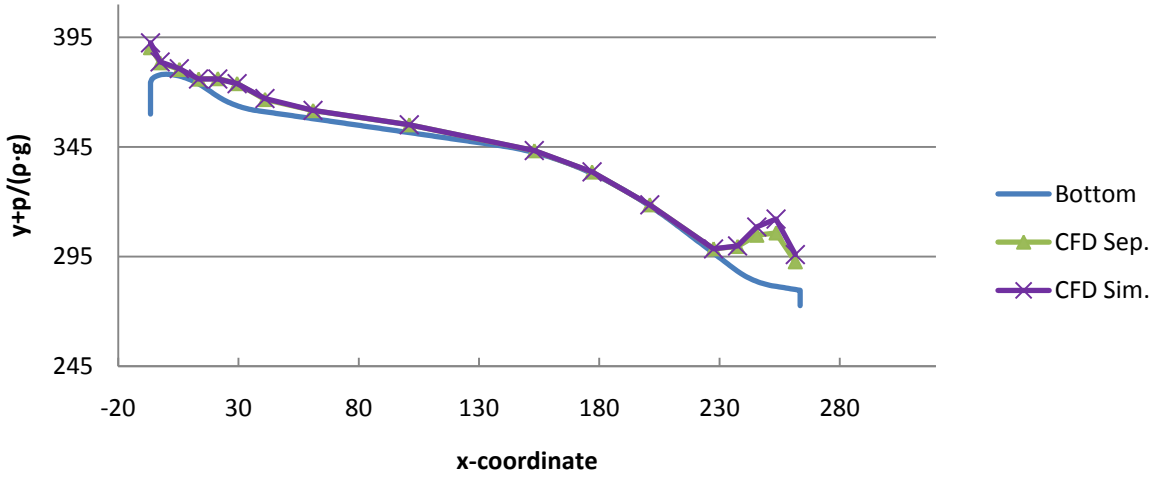

10000 m^3/s		Channel 2
	CFD one channel separately	CFD five channels simultaneously
Point	p (kPa)	p (kPa)
1	180,2	209,7
2	52,3	56,5
3	27,3	31,6
4	26,5	27,4
5	104,5	102,2
6	132,3	131,7
7	82,1	86,1
8	50,0	50,7
9	47,0	46,6
10	9,5	10,3
11	7,2	8,0
12	5,9	6,0
13	28,0	27,9
14	176,5	184,8
15	314,1	364,0
16	337,8	412,0
17	161,2	194,7

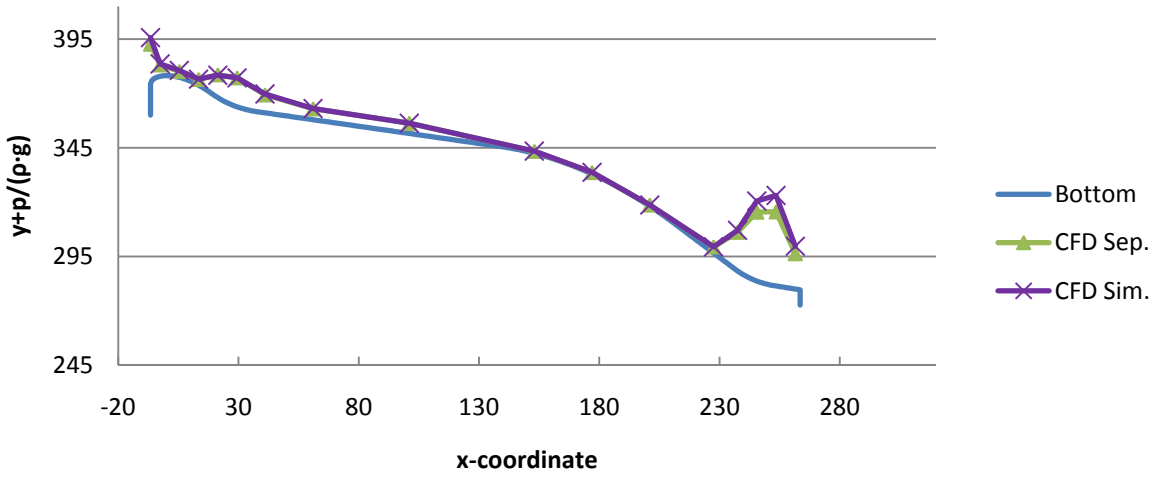

11940 m^3/s		Channel 2
	CFD one channel separately	CFD five channels simultaneously
Point	p (kPa)	p (kPa)
1	194,2	228,4
2	48,6	53,7
3	25,1	30,2
4	30,3	31,1
5	119,7	116,2
6	152,3	150,4
7	101,3	104,1
8	59,6	59,6
9	54,9	54,0
10	10,0	10,7
11	7,2	8,1
12	6,0	6,1
13	36,5	36,2
14	230,2	242,0
15	382,2	436,4
16	399,1	469,0
17	187,5	213,5

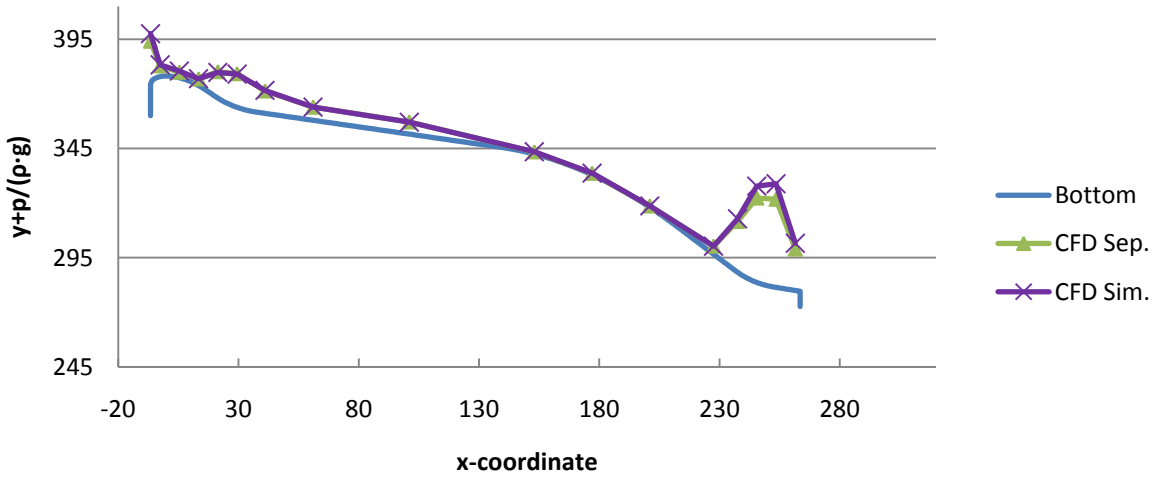

14810 m^3/s		Channel 2
	CFD one channel separately	CFD five channels simultaneously
Point	p (kPa)	p (kPa)
1	212,4	250,3
2	40,9	50,0
3	21,7	28,5
4	36,7	36,1
5	140,1	132,2
6	178,6	171,2
7	129,5	126,0
8	74,4	70,6
9	66,3	62,8
10	10,4	10,9
11	6,9	8,0
12	5,8	6,2
13	56,2	50,5
14	316,9	319,3
15	468,3	514,2
16	484,0	527,1
17	219,3	233,3

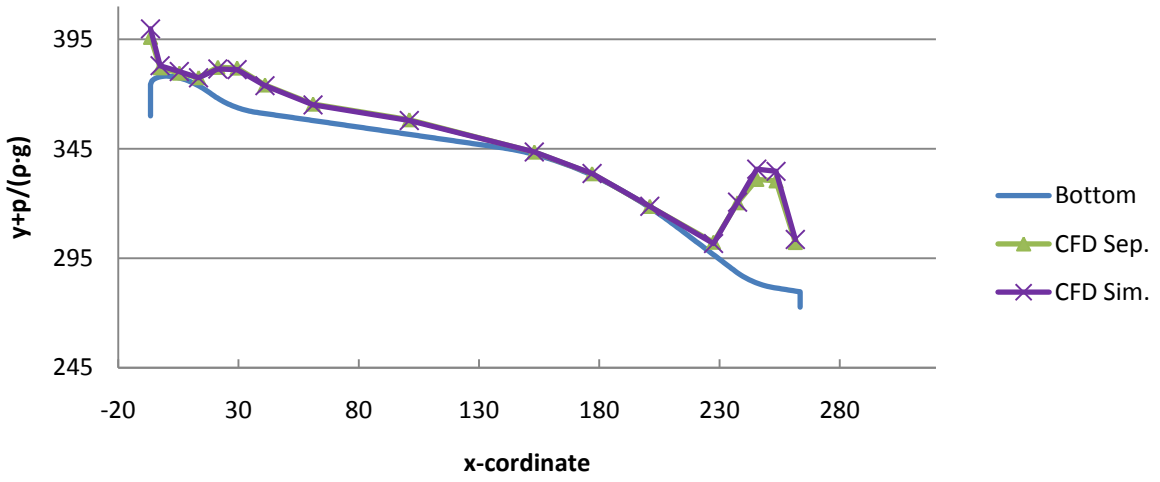

Channel 3

7240 m^3/s					Channel 3
	Exp. Data	CFD one channel separately		CFD five channels simultaneously	
Point	p (kPa)	p (kPa)	$\Delta p/p_{exp}$	p (kPa)	$\Delta p/p_{exp}$
1	130,4	157,0	20%	178,6	37%
2	78,2	55,0	-30%	58,4	-25%
3	28,4	30,1	6%	33,3	17%
4	2,7	21,9	707%	22,1	716%
5	28,3	80,6	185%	78,5	177%
6	10,8	100,0	826%	99,3	820%
7	14,4	55,7	287%	59,5	314%
8	10,1	36,9	263%	37,5	269%
9	19,3	35,5	84%	35,0	81%
10	11,8	8,6	-28%	9,3	-21%
11	13,0	6,8	-48%	7,3	-44%
12	12,4	5,5	-56%	5,6	-55%
13	14,9	18,1	22%	16,1	8%
14	78,4	117,6	50%	112,8	44%
15	200,2	232,6	16%	239,4	20%
16	298,6	289,7	-3%	292,7	-2%
17	214,0	174,1	-19%	165,3	-23%

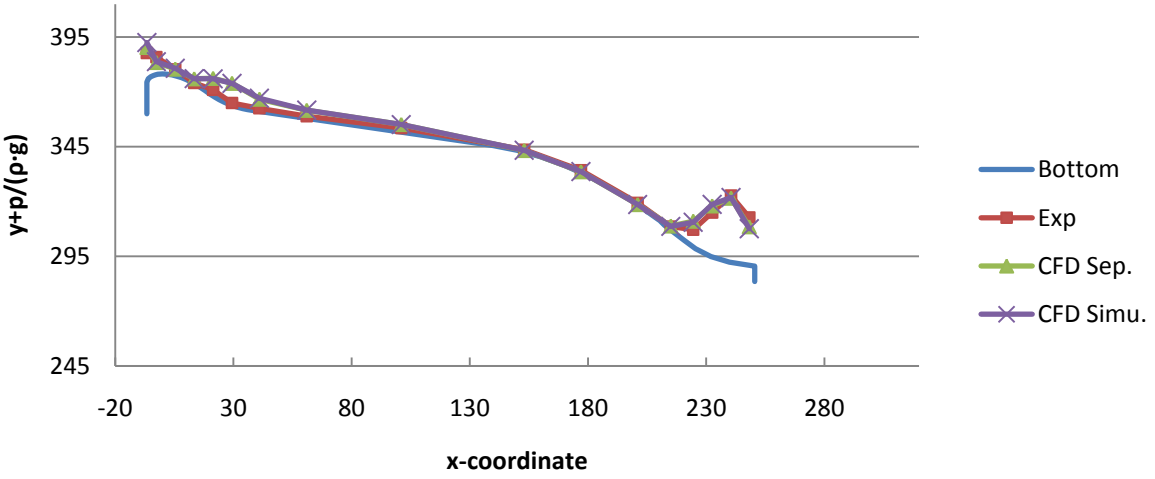

10000 m^3/s					Channel 3
	Exp. Data	CFD one channel separately		CFD five channels simultaneously	
Point	p (kPa)	p (kPa)	$\Delta p/p_{exp}$	p (kPa)	$\Delta p/p_{exp}$
1	105,9	180,0	70%	209,3	98%
2	69,4	52,2	-25%	56,5	-19%
3	5,9	27,3	364%	31,8	440%
4	13,5	26,6	97%	27,5	104%
5	60,6	104,5	72%	101,9	68%
6	32,3	132,3	309%	131,4	306%
7	13,4	82,1	513%	86,0	541%
8	14,1	50,0	256%	50,6	260%
9	-0,3	47,0	-	46,5	-
10	32,4	9,5	-71%	10,3	-68%
11	18,9	7,3	-61%	8,0	-58%
12	4,6	5,9	29%	6,0	32%
13	11,0	26,9	145%	24,5	123%
14	172,3	195,5	13%	184,1	7%
15	330,4	349,0	6%	352,2	7%
16	416,1	389,7	-6%	392,1	-6%
17	253,2	218,5	-14%	202,2	-20%

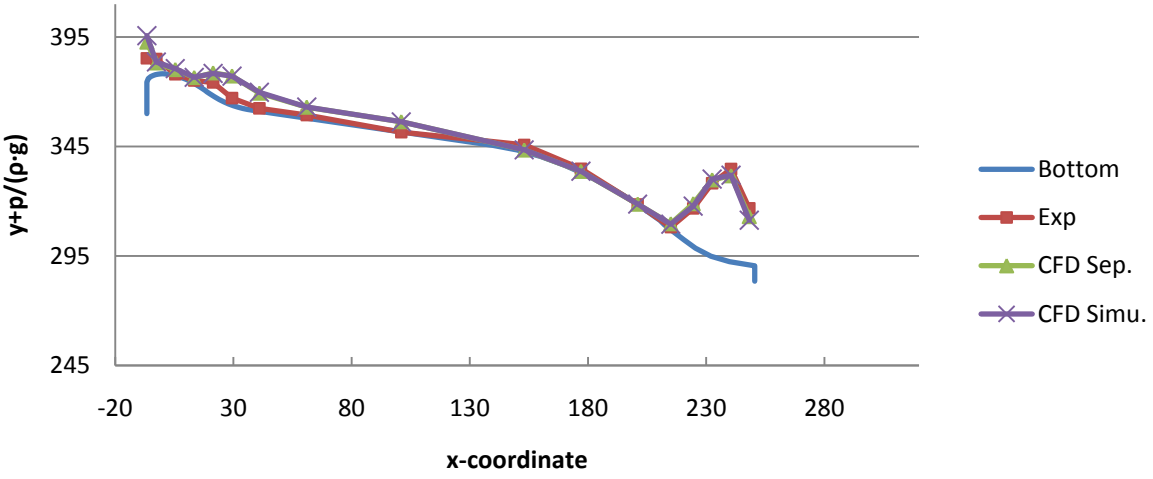

11940 m^3/s					Channel 3
	Exp. Data	CFD one channel separately		CFD five channels simultaneously	
Point	p (kPa)	p (kPa)	$\Delta p/p_{exp}$	p (kPa)	$\Delta p/p_{exp}$
1	134,3	194,1	44%	227,8	70%
2	39,1	48,5	24%	53,5	37%
3	4,9	25,1	411%	30,5	521%
4	24,3	30,3	25%	31,4	29%
5	78,2	119,7	53%	116,0	48%
6	51,9	152,3	193%	150,1	189%
7	15,4	101,3	559%	104,0	577%
8	0,4	59,6	16806%	59,5	16770%
9	10,5	54,9	424%	53,9	414%
10	11,8	10,0	-15%	10,7	-9%
11	16,0	7,4	-54%	8,1	-49%
12	22,2	6,0	-73%	6,2	-72%
13	40,3	37,5	-7%	33,2	-18%
14	236,0	261,8	11%	241,7	2%
15	389,1	417,1	7%	420,0	8%
16	499,3	450,7	-10%	444,2	-11%
17	277,7	246,6	-11%	221,5	-20%

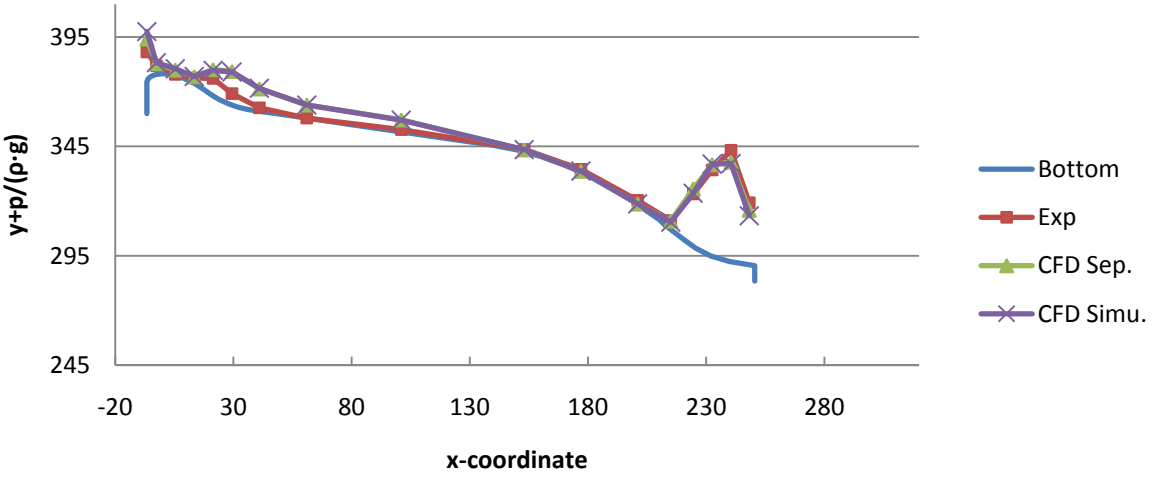

14810 m^3/s					Channel 3
	Exp. Data	CFD one channel separately		CFD five channels simultaneously	
Point	p (kPa)	p (kPa)	$\Delta p/p_{exp}$	p (kPa)	$\Delta p/p_{exp}$
1	67,7	212,2	213%	249,7	269%
2	33,2	40,9	23%	49,6	50%
3	27,4	21,7	-21%	28,7	5%
4	43,8	36,7	-16%	36,3	-17%
5	100,7	140,1	39%	132,0	31%
6	53,9	178,6	231%	170,9	217%
7	4,6	129,5	2720%	125,8	2640%
8	1,3	74,4	5485%	70,5	5194%
9	0,7	66,3	9441%	62,7	8915%
10	3,0	10,4	246%	11,0	263%
11	23,8	7,0	-70%	8,0	-66%
12	-15,0	6,1	-	6,3	-
13	128,5	67,4	-48%	49,5	-61%
14	336,8	363,8	8%	317,6	-6%
15	462,6	491,3	6%	491,1	6%
16	563,0	533,0	-5%	497,4	-12%
17	297,2	275,5	-7%	242,4	-18%

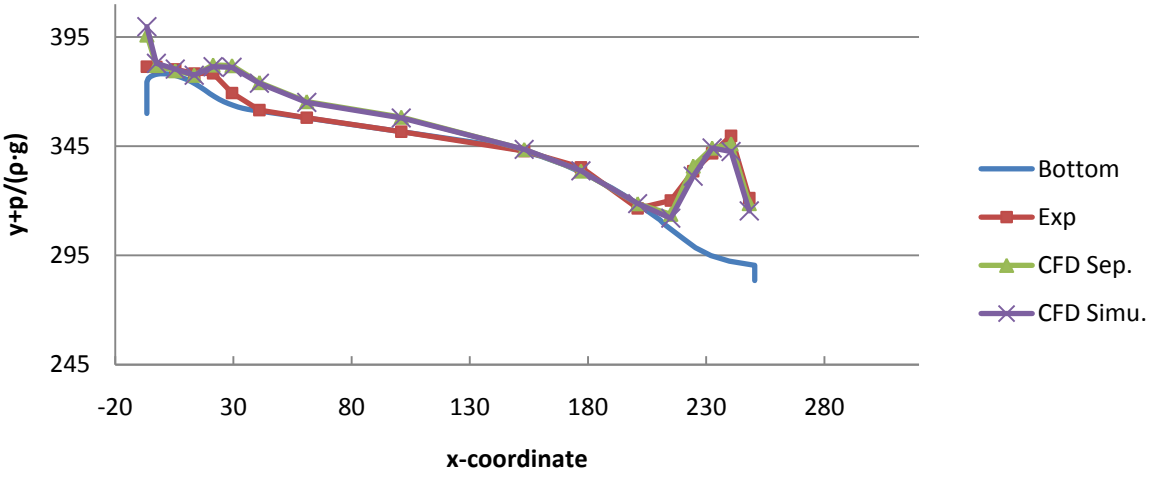

Channel 4

7240 m^3/s		Channel 4
	CFD one channel separately	CFD five channels simultaneously
Point	p (kPa)	p (kPa)
1	157,1	178,8
2	55,1	58,2
3	30,1	33,2
4	21,9	22,1
5	80,6	78,3
6	100,0	99,0
7	55,7	59,3
8	36,8	37,3
9	35,5	34,8
10	8,6	9,3
11	6,2	7,1
12	-0,4	4,2
13	32,2	16,2
14	98,4	96,1
15	230,5	234,0
16	281,0	282,2
17	153,1	144,4

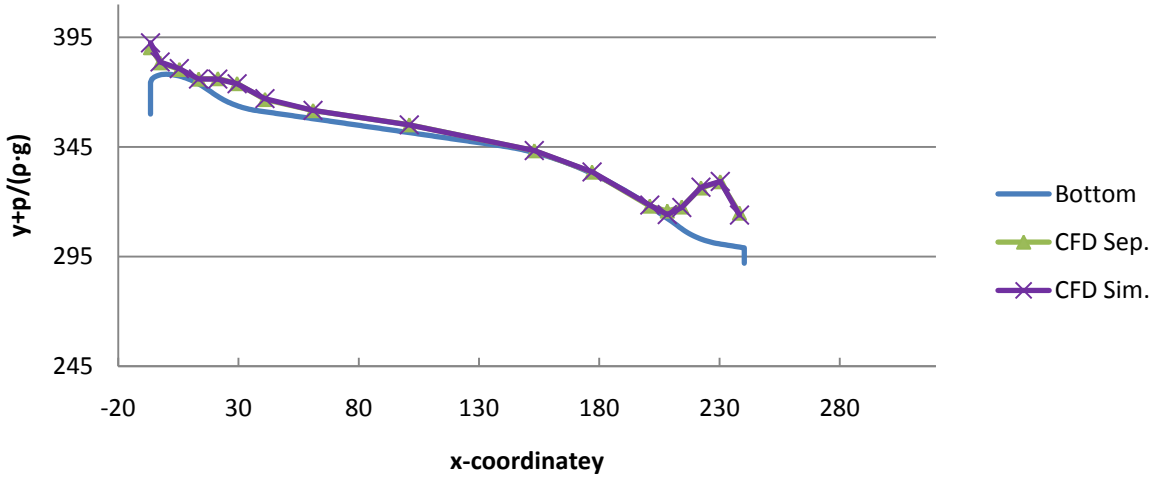

10000 m^3/s		Channel 4
	CFD one channel separately	CFD five channels simultaneously
Point	p (kPa)	p (kPa)
1	180,2	209,6
2	52,3	56,5
3	27,3	31,6
4	26,5	27,3
5	104,5	102,2
6	132,3	130,8
7	82,1	85,4
8	50,0	50,4
9	47,0	46,3
10	9,5	10,2
11	6,7	7,7
12	0,3	5,3
13	53,4	33,3
14	176,7	166,0
15	339,5	340,8
16	372,8	373,7
17	188,9	174,7

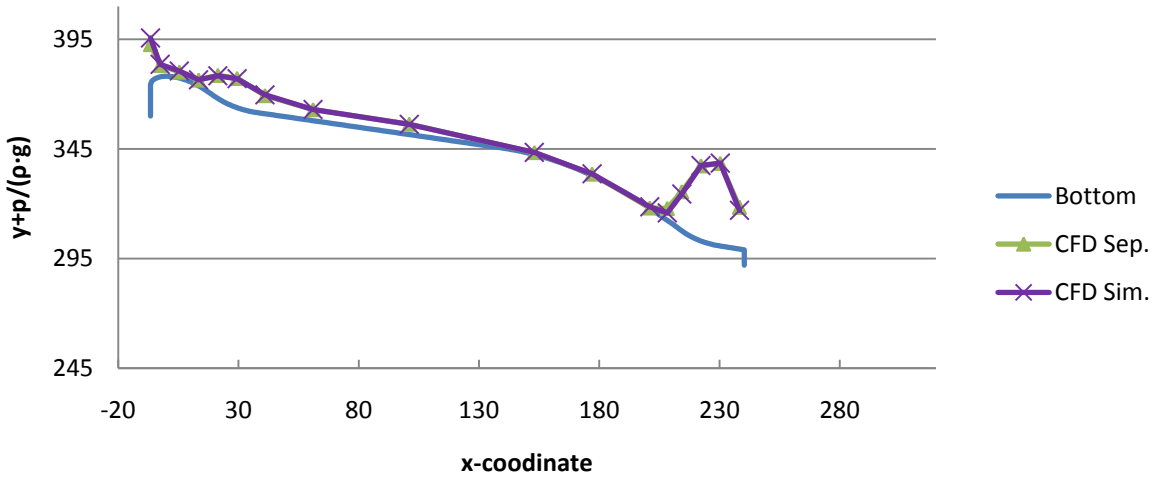

11940 m^3/s		Channel 4
	CFD one channel separately	CFD five channels simultaneously
Point	p (kPa)	p (kPa)
1	194,2	228,1
2	48,6	53,4
3	25,1	30,1
4	30,3	31,0
5	119,7	115,3
6	152,3	149,3
7	101,3	103,1
8	59,6	59,0
9	54,9	53,5
10	10,0	10,6
11	6,6	7,8
12	2,6	6,9
13	80,7	52,8
14	244,0	222,0
15	399,8	402,8
16	425,5	421,2
17	211,1	190,6

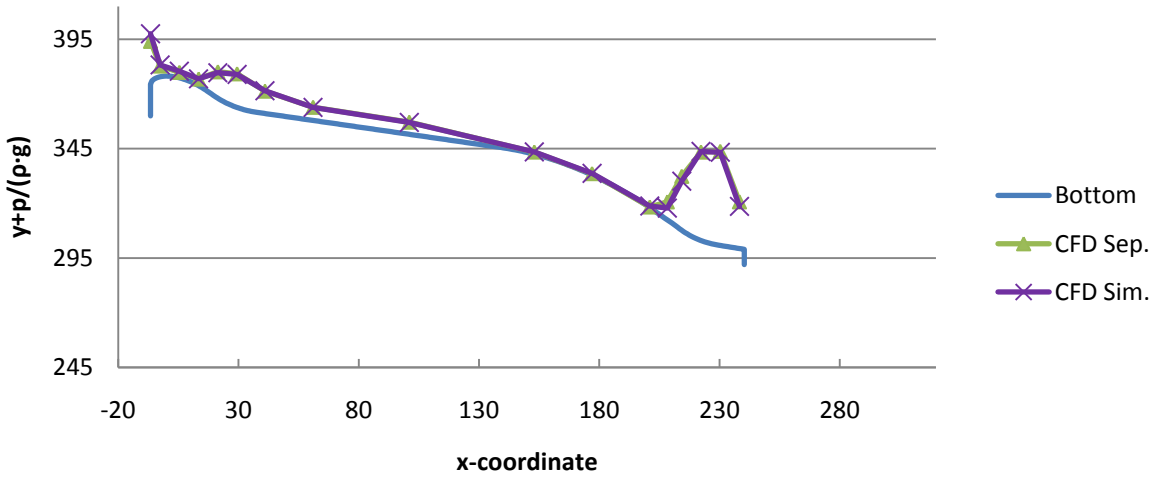

14810 m^3/s		Channel 4
	CFD one channel separately	CFD five channels simultaneously
Point	p (kPa)	p (kPa)
1	212,4	249,4
2	40,9	48,8
3	21,7	28,4
4	36,7	36,0
5	140,1	131,4
6	178,6	170,1
7	129,5	125,1
8	74,4	70,1
9	66,3	62,4
10	10,3	10,9
11	6,2	7,8
12	14,4	11,2
13	157,0	89,2
14	337,4	296,4
15	451,6	468,2
16	477,6	470,7
17	223,1	209,1

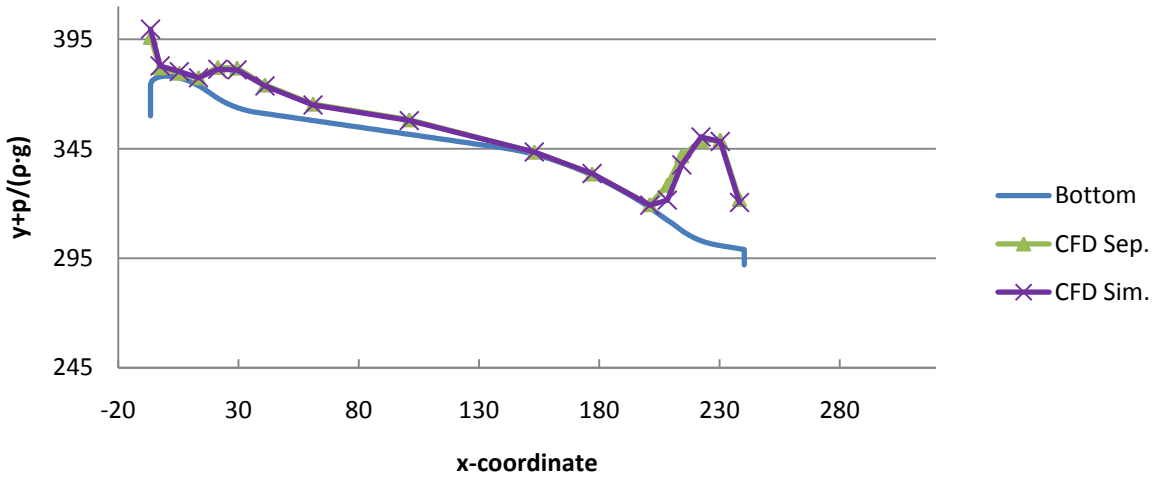

1.1.

Channel 5

7240 m^3/s					Channel 5
	Exp. Data	CFD one channel separately		CFD five channels simultaneously	
Point	p (kPa)	p (kPa)	$\Delta p/p_{exp}$	p (kPa)	$\Delta p/p_{exp}$
1	128,4	156,1	22%	178,4	39%
2	184,0	55,0	-70%	58,4	-68%
3	20,6	30,1	46%	33,0	60%
4	29,1	21,9	-25%	22,0	-25%
5	29,7	80,5	171%	78,2	164%
6	7,3	100,2	1278%	99,0	1261%
7	23,6	55,6	136%	59,3	151%
8	18,7	35,5	90%	34,9	86%
9	39,6	8,5	-78%	9,3	-76%
10	6,6	7,0	7%	7,5	14%
11	33,4	4,3	-87%	4,7	-86%
12	23,0	15,5	-33%	15,1	-34%
13	46,6	69,6	49%	68,1	46%
14	202,4	224,7	11%	226,4	12%
15	292,1	268,3	-8%	270,3	-7%
16	188,4	142,5	-24%	135,0	-28%

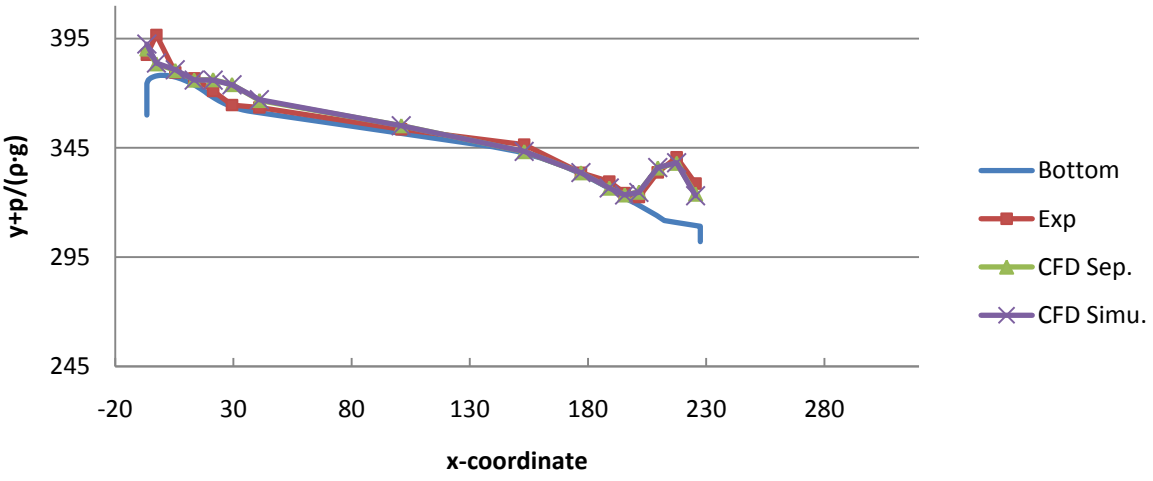

10000 m^3/s					Channel 5
	Exp. Data	CFD one channel separately		CFD five channels simultaneously	
Point	p (kPa)	p (kPa)	$\Delta p/p_{exp}$	p (kPa)	$\Delta p/p_{exp}$
1	148,0	178,7	21%	209,1	41%
2	131,1	52,2	-60%	56,6	-57%
3	0,0	27,3	278794%	31,3	319242%
4	8,6	26,5	209%	27,2	217%
5	63,0	104,3	66%	101,5	61%
6	100,3	132,6	32%	130,8	30%
7	51,0	82,1	61%	85,4	67%
8	16,8	47,0	181%	46,3	176%
9	39,6	9,5	-76%	10,3	-74%
10	23,2	7,6	-67%	8,2	-65%
11	44,2	6,1	-86%	6,4	-85%
12	20,1	34,6	73%	31,4	56%
13	44,7	144,6	224%	131,1	193%
14	114,3	321,8	182%	324,7	184%
15	393,9	348,7	-11%	352,4	-11%
16	210,9	172,8	-18%	162,4	-23%

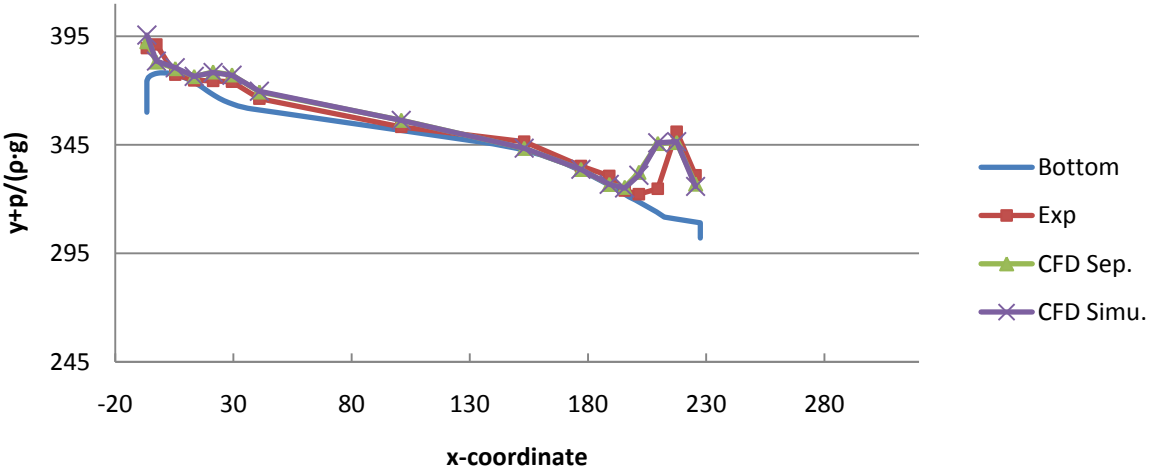

11940 m^3/s					Channel 5
	Exp. Data	CFD one channel separately		CFD five channels simultaneously	
Point	p (kPa)	p (kPa)	$\Delta p/p_{exp}$	p (kPa)	$\Delta p/p_{exp}$
1	148,0	192,4	30%	228,0	54%
2	147,7	48,5	-67%	54,1	-63%
3	22,5	25,0	11%	29,5	31%
4	15,4	30,2	96%	30,6	98%
5	76,7	119,4	56%	115,2	50%
6	101,3	152,6	51%	149,2	47%
7	77,4	101,3	31%	97,7	26%
8	36,3	54,9	51%	53,5	47%
9	39,6	9,9	-75%	10,6	-73%
10	47,7	7,8	-84%	8,5	-82%
11	53,0	9,9	-81%	9,1	-83%
12	25,9	61,5	137%	50,5	95%
13	222,8	210,4	-6%	183,0	-18%
14	320,9	372,6	16%	379,2	18%
15	430,1	392,8	-9%	394,3	-8%
16	223,7	190,3	-15%	176,7	-21%

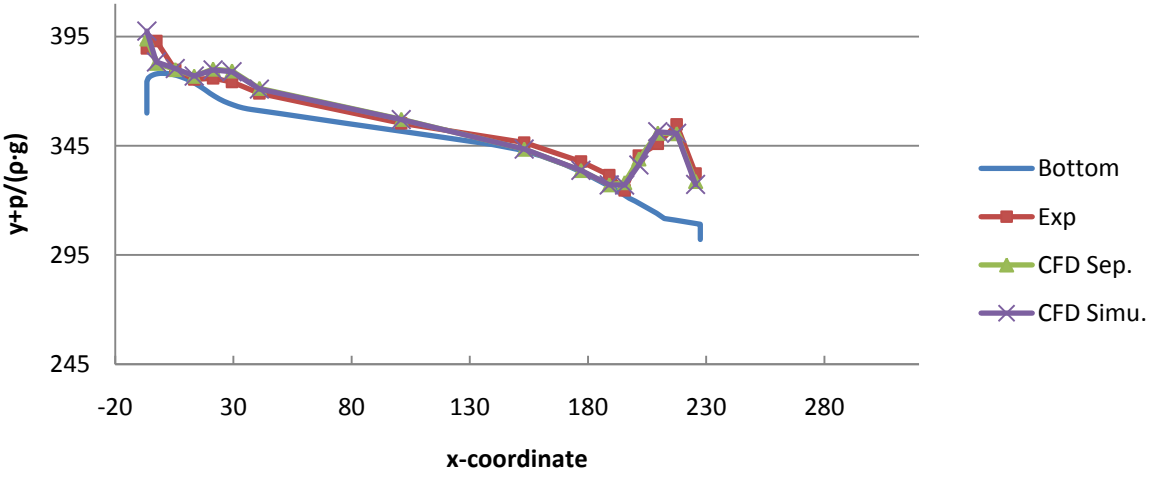

14810 m^3/s					Channel 5
	Exp. Data	CFD one channel separately		CFD five channels simultaneously	
Point	p (kPa)	p (kPa)	$\Delta p/p_{exp}$	p (kPa)	$\Delta p/p_{exp}$
1	81,5	210,0	158%	249,2	206%
2	75,3	40,8	-46%	49,7	-34%
3	28,4	21,7	-24%	27,5	-3%
4	-6,1	36,5	-	35,2	-
5	46,3	139,7	202%	130,7	182%
6	123,8	179,0	45%	169,4	37%
7	99,9	129,5	30%	124,2	24%
8	-0,9	66,3	-	62,1	-
9	39,6	10,3	-74%	10,9	-73%
10	6,6	7,9	20%	8,6	31%
11	89,2	24,6	-72%	15,4	-83%
12	57,3	126,7	121%	84,1	47%
13	90,7	305,8	237%	250,5	176%
14	374,7	424,6	13%	434,2	16%
15	455,6	443,6	-3%	436,5	-4%
16	233,5	210,2	-10%	193,2	-17%

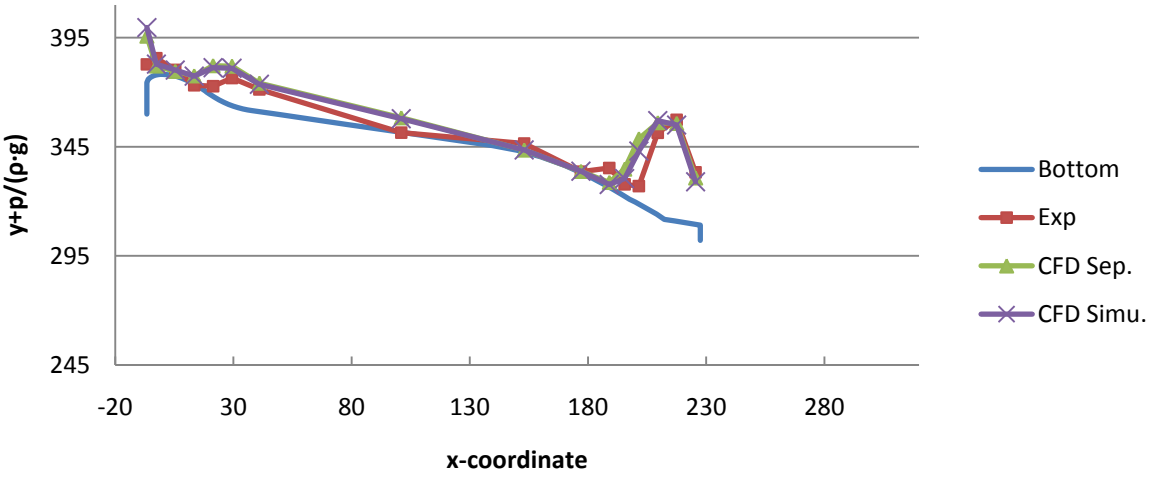

APPENDIX C – ANALYTICAL DETERMINATION OF PRESSURE

2 pages

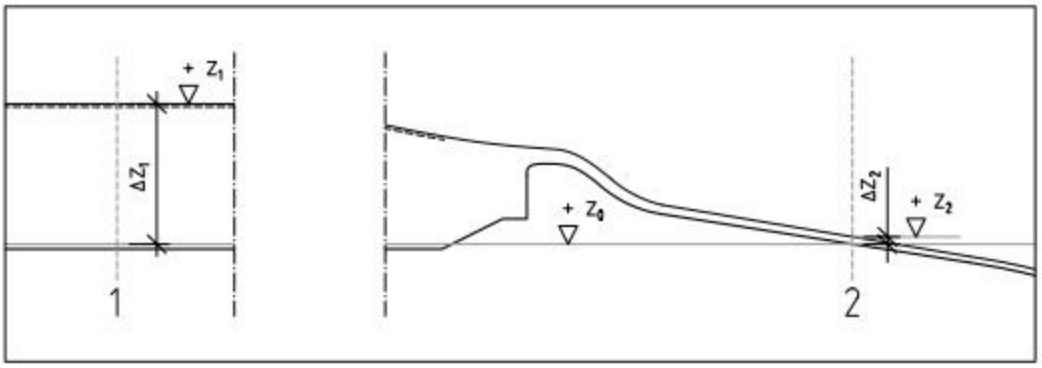

The energy equation

$$\Delta z_1 + \frac{v_1^2}{2g} + \frac{p_1}{\rho \cdot g} = \Delta z_2 + \frac{v_2^2}{2g} + \frac{p_2}{\rho \cdot g} + \Sigma h$$

Simplifications

The assumption is made that no velocity exist in section 1, the section is placed in the reservoir.

The pressure at section 1 and 2 are assumed to be equal (atmospheric pressure) and will therefore be removed from the equation.

This analytical determination of the water depth in section 2 is just a simple control and therefore no head losses are considered.

Resulting equation:

$$\Delta z_1 = \Delta z_2 + \frac{v_2^2}{2g}$$

where:

$$v_2 = \frac{Q_2}{A_2 \cdot 2g} = \frac{Q_2}{\left(b_2 \cdot \Delta z_2\right) \cdot 2g} \qquad \textbf{and} \qquad \Delta z_1 = z_1 - z_0 \qquad \Delta z_2 = z_2 - z_0$$

which leads to:

$$\left(z_1 - z_0\right) = \left(z_2 - z_0\right) + \frac{Q_2^2}{\left[b_2 \cdot \left(z_2 - z_0\right)\right]^2 \cdot 2g}$$

This expression is an equation of the third degree and can be solved numerically using, for example, Mathcad.

The first section is, as mentioned before, located far upstream. The second section is located at measuring point 8 in Channel 3.

Input

$z_0 := 357.904\text{m}$ The vertical coordinate for measuring point 8 in Channel 3.

$z_1 := 398.000\text{m}$ The unaffected upstream water level from the scale model. tests for the discharge Q=11 940 m^3/s.

$z_2 := 363.000\text{m}$ Initial value for z_2, this input is needed in the numerical solution.

$Q_2 := 2388 \frac{m^3}{s}$ The flow in Channel 3 (one fifth of the total flow).

$b_2 := 16\text{m}$ The bredth of Channel 3 at measuring point 8.

$g = 9.807 \frac{m}{s^2}$ The gravitational constant.

$\rho_w := 1000 \frac{kg}{m^3}$ Approximation of the water density.

Solving

Given Mathcad algorithm for numerical solving

$$(z_1 - z_0) = (z_2 - z_0) + \frac{{Q_2}^2}{\left[b_2 \cdot (z_2 - z_0)\right]^2 \cdot 2g}$$

$z_2 := \text{Find}(z_2)$ The analytical elevation of the water surface at point 8 in Channel 3. $z_2 = 363.654\,\text{m}$

$\Delta z_2 := z_2 - z_0$ The analytical water depth at measuring point 8 in Channel 3. $\Delta z_2 = 5.75\,\text{m}$

$p := \rho_w \cdot g \cdot \Delta z_2$ The analytical pressure at measuring point 8 based on the assumption that the stream lines are parallell with the bottom and the walls, i.e. hydrostatic conditions occur. $p = 56.393 \cdot \text{kPa}$

APPENDIX D – FAULT TREE

1 page

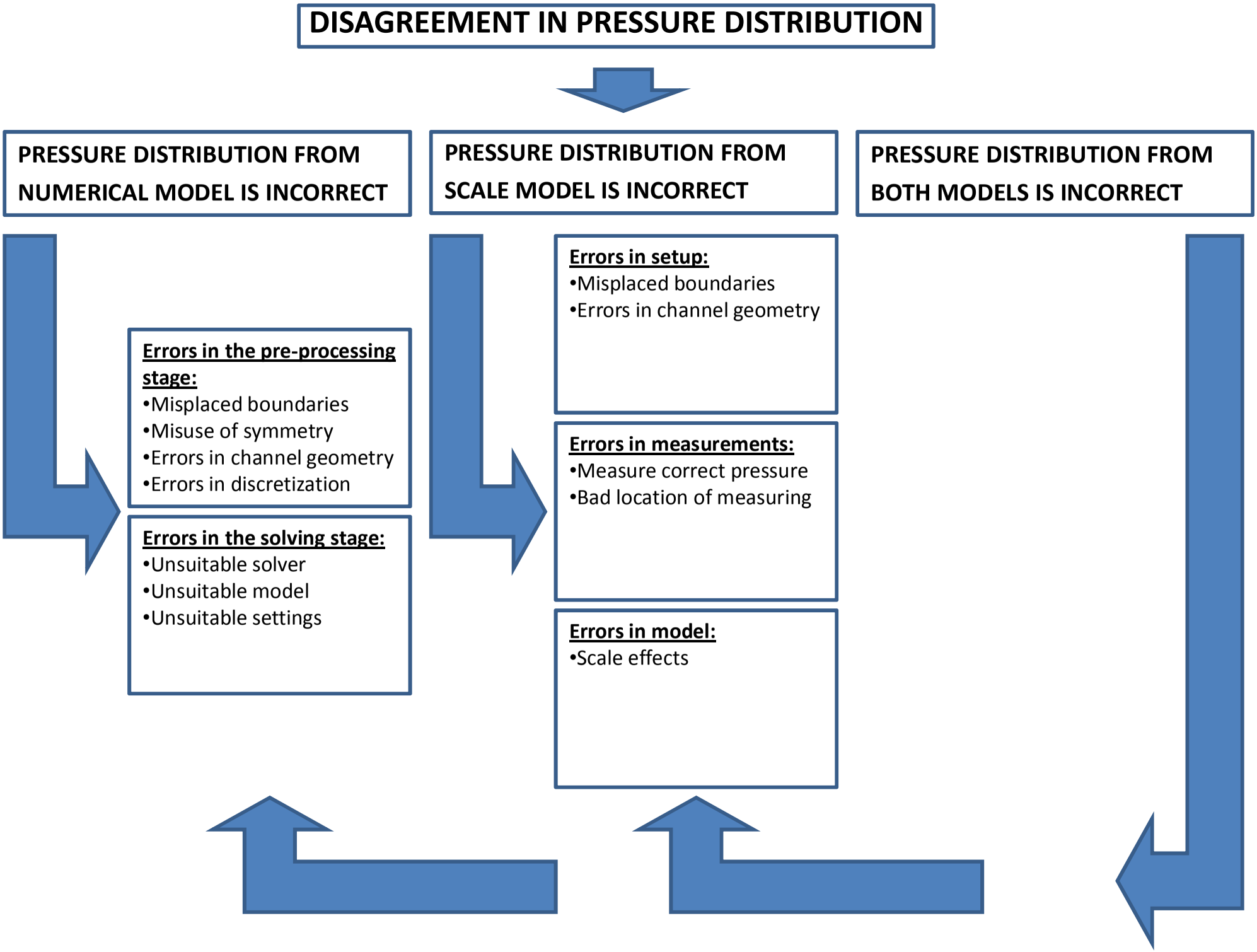
DISAGREEMENT IN PRESSURE DISTRIBUTION
PRESSURE DISTRIBUTION FROM NUMERICAL MODEL IS INCORRECT
PRESSURE DISTRIBUTION FROM SCALE MODEL IS INCORRECT
PRESSURE DISTRIBUTION FROM BOTH MODELS IS INCORRECT
Errors in the pre-processing stage:
•Misplaced boundaries
•Misuse of symmetry
•Errors in channel geometry
•Errors in discretization
Errors in the solving stage:
•Unsuitable solver
•Unsuitable model
•Unsuitable settings
Errors in setup:
•Misplaced boundaries
•Errors in channel geometry
Errors in measurements:
•Measure correct pressure
•Bad location of measuring
Errors in model:
•Scale effects